

Q -fully quadratic modeling and its application in a random subspace derivative-free method

Yiwen Chen · Warren Hare · Amy Wiebe

December 7, 2023

Abstract Model-based derivative-free optimization (DFO) methods are an important class of DFO methods that are known to struggle with solving high-dimensional optimization problems. Recent research has shown that incorporating random subspaces into model-based DFO methods has the potential to improve their performance on high-dimensional problems. However, most of the current theoretical and practical results are based on linear approximation models due to the complexity of quadratic approximation models. This paper proposes a random subspace trust-region algorithm based on quadratic approximations. Unlike most of its precursors, this algorithm does not require any special form of objective function. We study the geometry of sample sets, the error bounds for approximations, and the quality of subspaces. In particular, we provide a technique to construct Q -fully quadratic models, which is easy to analyze and implement. We present an almost-sure global convergence result of our algorithm and give an upper bound on the expected number of iterations to find a sufficiently small gradient. We also develop numerical experiments to compare the performance of our algorithm using both linear and quadratic approximation models. The numerical results demonstrate the strengths and weaknesses of using quadratic approximations.

1 Introduction

Derivative-free optimization (DFO) methods are a class of optimization methods that do not use the derivatives of the objective or constraint functions [4, 12]. In recent years, DFO has continued to gain popularity and has demonstrated effective use in solving optimization problems where the derivative information is expensive or impossible to obtain. Such problems occur regularly in many fields of modern research. For example, the objective or constraints may be given by computer simulation or laboratory experiments. A recent survey of the applications of DFO methods can be found in [1], in which the authors review hundreds of applications of DFO methods and particularly focus on energy, materials science, and computational engineering design. More recently, with the emergence of artificial intelligence, large-scale DFO methods

Department of Mathematics, University of British Columbia, Kelowna, British Columbia, V1V 1V7, Canada.
This research is partially funded by the Natural Sciences and Engineering Research Council of Canada (cette recherche est partiellement financée par le Conseil de recherches en sciences naturelles et en génie du Canada), Discover Grant #2023-03555 and by the Mitacs Globalink Graduate Fellowship.
E-mail: yiwchen@student.ubc.ca, warren.hare@ubc.ca, amy.wiebe@ubc.ca

have gained attention as they have great potential to handle problems such as hyperparameter tuning [16, 18, 27] and generating attacks to deep neural networks [2, 7].

One major class of DFO methods is model-based methods [5, 26, 28]. In model-based DFO methods, model functions are constructed iteratively to approximate the objective and constraint functions. Unfortunately, most of the current model-based DFO methods are inefficient in high dimensions, since both the number of function evaluations and the linear algebra cost required to construct models increase with the problem dimension.

One promising technique to handle large optimization problems is through subspaces. This technique has long been used in gradient-based optimization [13, 17, 20] and more recently been applied in DFO [3, 35]. Audet et al. [3] apply a parallel space decomposition technique and introduce an asynchronous parallel generalized pattern search algorithm in which each processor solves the optimization problem over only a subset of variables. In [35], Zhang proposes a subspace trust-region method based on NEWUOA [31, 32]. Numerical results demonstrate a significant improvement over NEWUOA on large-scale problems. More recently, randomization is being incorporated by working in low-dimensional subspaces that are chosen randomly in each iteration [6, 15, 24, 34]. Roberts and Royer [34] study a direct-search algorithm with search directions chosen in random subspaces. In [6] and [15], random subspace trust-region algorithms are proposed for solving nonlinear least-squares and stochastic optimization problems, respectively. The theoretical and numerical benefits of random subspaces are confirmed by the reduced per-iteration cost and strong performance of these algorithms. A theoretical analysis of the connection between the dimension of subspaces and the algorithmic performance can be found in [24].

All of the above random subspace trust-region algorithms only construct linear approximation models. This is because linear functions are easier to handle than quadratic functions in both theoretical analysis and computer programming aspects. Indeed, recall that a determined linear interpolation model in \mathbb{R}^n requires $(n + 1)$ sample points to construct, whereas a determined quadratic interpolation model requires $(n + 1)(n + 2)/2$ sample points [12]. This makes the geometry of sample sets, which is a key factor for model quality [10, 11], more difficult to manage in the quadratic case. Moreover, the only random subspace trust-region algorithm mentioned above developed for deterministic optimization is specialized to nonlinear least-squares problems. The algorithm proposed in [6] achieves scalability by exploring the special structure of the objective functions in nonlinear least-squares problems and is therefore not able to handle optimization problems with general objective functions.

This paper proposes a random subspace trust-region algorithm based on quadratic approximations for unconstrained deterministic optimization problems. This algorithm does not require the objective function to have any specific form (e.g., nonlinear least-squares) and is therefore able to handle a much broader scope of optimization problems. We provide rigorous theoretical analysis for model accuracy, sample set geometry, and subspace quality.

The sample set management procedure used in our algorithm is based on the condition number of the direction matrix corresponding to the sample set (see Subsection 2.3 for details). This is different from the management procedures used in most of the previous algorithms, which are based on the Lagrange polynomials. We note that our procedure is easier for managing quadratic interpolation sample sets than the procedure based on Lagrange polynomials from [6]. This is because the Lagrange polynomial approach requires maximizing quadratic functions over balls.

We prove the almost-sure global convergence of our algorithm and give a complexity bound on the expected number of iterations required to find a sufficiently small gradient. By numerical experiments, we demonstrate the advantages and disadvantages of quadratic models over linear models and the benefits of exploring the structure of objective functions when possible.

It is worth mentioning that most of the theoretical results given in this paper are independent of the algorithm. In particular, our Q -fully quadratic modeling technique is easy to handle for

both theoretical analysis and implementation purposes and constructs a class of models that is more accurate than required to prove convergence (see Subsection 2.4 and Section 3 for details). Therefore, this paper also provides several theoretical tools for future DFO algorithm design.

The remainder of this paper is organized as follows. We end this section with remarks on our notation. In Section 2, we describe the general framework of our algorithm and explain our model construction technique, sample set management procedure, and subspace selection strategy. In Section 3, we provide the convergence analysis of our algorithm. In Section 4, we design numerical experiments to compare the performance of our algorithm based on quadratic and linear models. Section 5 concludes our work and gives some suggestions for future work.

1.1 Notation and background definitions

We work in Euclidean space \mathbb{R}^n , with inner product $x^\top y = \sum_{i=1}^n x_i y_i$ and induced vector norm $\|x\| = \sqrt{x^\top x}$. For a matrix $A \in \mathbb{R}^{n \times z}$, we use the induced matrix norm $\|A\| = \max\{\|Ax\| : x \in \mathbb{R}^z, \|x\| = 1\}$. The ij -th element of A is denoted by A_{ij} . Functions $\lambda_{\min}(\cdot)$ and $\sigma_{\min}(\cdot)$ give the minimum eigenvalue and singular value of a matrix, respectively. We use $A = [a_1 \cdots a_z]$ to denote the column representation of A and we write $a_i \in A$ to mean that vector a_i is a column of A . We use I_n to denote the identity matrix of order n . For $i \in \{1, \dots, n\}$, we use $e_i^{(n)} \in \mathbb{R}^n$ to denote the i -th column of I_n , i.e., the i -th coordinate vector in \mathbb{R}^n . For a set S , we use $|S|$ to denote the cardinality of S . The set $B(x; \Delta)$ is the closed ball centered at x with radius Δ :

$$B(x; \Delta) = \{y : \|y - x\| \leq \Delta\}.$$

For an invertible square matrix $A \in \mathbb{R}^{n \times n}$, we denote the inverse of A by A^{-1} . Also, we use a generalization of the inverse matrix called the Moore–Penrose Pseudoinverse [30].

Definition 1 (*Moore–Penrose Pseudoinverse*) For a matrix $A \in \mathbb{R}^{n \times z}$, the Moore–Penrose Pseudoinverse of A , denoted by A^\dagger , is the unique matrix in $\mathbb{R}^{z \times n}$ satisfying the following four conditions:

1. $AA^\dagger A = A$,
2. $A^\dagger AA^\dagger = A^\dagger$,
3. $(AA^\dagger)^\top = AA^\dagger$,
4. $(A^\dagger A)^\top = A^\dagger A$.

Note that A^\dagger exists and is unique for any matrix $A \in \mathbb{R}^{n \times z}$ [30]. In particular, when A has full rank, A^\dagger can be expressed by the following simple formulae [30].

1. If $A \in \mathbb{R}^{n \times z}$ has full column rank z , then A^\dagger is a left-inverse of A , i.e., $A^\dagger A = I_z$ and

$$A^\dagger = (A^\top A)^{-1} A^\top.$$

2. If $A \in \mathbb{R}^{n \times z}$ has full row rank n , then A^\dagger is a right-inverse of A , i.e., $AA^\dagger = I_n$ and

$$A^\dagger = A^\top (AA^\top)^{-1}.$$

Now we introduce the generalized simplex gradient [22] and the generalized simplex Hessian [23]. We note that the generalized simplex Hessian we define below is a special case of the definition given in [23].

Definition 2 (Generalized simplex gradient) Let $x^0 \in \mathbb{R}^n$ and $D = [d_1 \cdots d_z] \in \mathbb{R}^{n \times z}$. The generalized simplex gradient of f at x^0 over D , denoted by $\nabla_S f(x^0; D)$, is defined by

$$\nabla_S f(x^0; D) = (D^\top)^\dagger \delta_f(x^0; D),$$

where

$$\delta_f(x^0; D) = \begin{bmatrix} f(x^0 + d_1) - f(x^0) \\ f(x^0 + d_2) - f(x^0) \\ \vdots \\ f(x^0 + d_z) - f(x^0) \end{bmatrix}. \quad (1)$$

Definition 3 (Generalized simplex Hessian) Let $x^0 \in \mathbb{R}^n$ and $D = [d_1 \cdots d_z] \in \mathbb{R}^{n \times z}$. The generalized simplex Hessian of f at x^0 over D , denoted by $\nabla_S^2 f(x^0; D)$, is defined by

$$\nabla_S^2 f(x^0; D) = (D^\top)^\dagger \delta_{\nabla_S f}(x^0; D),$$

where

$$\delta_{\nabla_S f}(x^0; D) = \begin{bmatrix} (\nabla_S f(x^0 + d_1; D) - \nabla_S f(x^0; D))^\top \\ (\nabla_S f(x^0 + d_2; D) - \nabla_S f(x^0; D))^\top \\ \vdots \\ (\nabla_S f(x^0 + d_z; D) - \nabla_S f(x^0; D))^\top \end{bmatrix}. \quad (2)$$

2 Quadratic approximation random subspace trust-region algorithm

This section introduces our Quadratic Approximation Random Subspace Trust-region Algorithm (QARSTA). We first explain how the interpolation models are constructed in QARSTA and analyze their accuracy. Then we outline the framework of QARSTA and discuss some important details. The convergence of QARSTA is proved in Section 3.

Throughout this section, we consider the objective function $f : \mathbb{R}^n \rightarrow \mathbb{R}$.

2.1 Model construction

The main idea of QARSTA is that, in each iteration, an interpolation model is constructed in a subspace of \mathbb{R}^n . This reduces the number of function evaluations and the computation effort to construct each model. Moreover, as pointed out in [6], since we do not capture the behaviors of the objective function outside our subspaces, this also improves the scalability of our algorithm.

In the k -th iteration of QARSTA, where the current iterate is x_k , we consider a p -dimensional affine space defined by

$$\mathcal{Y}_k = \{x_k + D_k \hat{s} : \hat{s} \in \mathbb{R}^p\},$$

where $D_k \in \mathbb{R}^{n \times p}$ has full-column rank.

Then, we construct a quadratic model that interpolates f in \mathcal{Y}_k . There are two equivalent ways to interpret this model: either as an underdetermined quadratic interpolation model in \mathbb{R}^n or as a determined quadratic interpolation model in \mathbb{R}^p . In this subsection, we explain how the model is constructed and how to convert between these two viewpoints.

The underdetermined quadratic model in \mathbb{R}^n is based on the generalized simplex gradient and generalized simplex Hessian.

Definition 4 Given $D = [d_1 \cdots d_p] \in \mathbb{R}^{n \times p}$ with full-column rank, $f : \mathbb{R}^n \rightarrow \mathbb{R}$, and $x^0 \in \mathbb{R}^n$. The model $m : \mathbb{R}^n \rightarrow \mathbb{R}$ is defined by

$$m(x) = f(x^0) + (2\nabla_S f(x^0; D) - \nabla_S f(x^0; 2D))^\top (x - x^0) + \frac{1}{2} (x - x^0)^\top \nabla_S^2 f(x^0; D) (x - x^0).$$

Theorem 1 The model $m(x)$ is an underdetermined quadratic interpolation model of f in \mathbb{R}^n . In particular, $m(x)$ interpolates $f(x)$ on all sample points in

$$Y = \{x^0\} \cup \{x^0 + d_i : i = 1, \dots, p\} \cup \{x^0 + d_i + d_j : i, j = 1, \dots, p\}.$$

Proof We only need to show that $m(x) = f(x)$ for all x in the set Y .

Case I: Suppose $x = x^0$. Then we have

$$m(x^0) = f(x^0) + (2\nabla_S f(x^0; D) - \nabla_S f(x^0; 2D))^\top \mathbf{0} + \frac{1}{2} \mathbf{0}^\top \nabla_S^2 f(x^0; D) \mathbf{0} = f(x^0).$$

Case II: Suppose $x = x^0 + d_i$ where $i \in \{1, \dots, p\}$. Since D has full-column rank, we have $D^\dagger D = I_p$. Therefore,

$$\nabla_S f(x^0; D)^\top D = \delta_f(x^0; D)^\top D^\dagger D = \delta_f(x^0; D)^\top,$$

$$\nabla_S f(x^0; 2D)^\top D = \delta_f(x^0; 2D)^\top (2D)^\dagger D = \frac{1}{2} \delta_f(x^0; 2D)^\top,$$

and

$$\nabla_S f(x^0 + d_i; D)^\top D = \delta_f(x^0 + d_i; D)^\top D^\dagger D = \delta_f(x^0 + d_i; D)^\top,$$

for all $i \in \{1, \dots, p\}$.

Based on these, we also have

$$D^\top \nabla_S^2 f(x^0; D) D = D^\top (D^\top)^\dagger \delta_{\nabla_S f(x^0; D)} D = \delta_{\nabla_S f(x^0; D)} D = \delta_{\delta_f(x^0; D)},$$

where

$$\delta_{\delta_f(x^0; D)} = \begin{bmatrix} (\delta_f(x^0 + d_1; D) - \delta_f(x^0; D))^\top \\ (\delta_f(x^0 + d_2; D) - \delta_f(x^0; D))^\top \\ \vdots \\ (\delta_f(x^0 + d_p; D) - \delta_f(x^0; D))^\top \end{bmatrix}. \quad (3)$$

Notice that for all $i \in \{1, \dots, p\}$, the i -th diagonal element of $\delta_{\delta_f(x^0; D)}$ is

$$f(x^0 + 2d_i) - 2f(x^0 + d_i) + f(x^0).$$

Hence, we obtain

$$\begin{aligned} & m(x^0 + d_i) \\ &= f(x^0) + (2\nabla_S f(x^0; D) - \nabla_S f(x^0; 2D))^\top d_i + \frac{1}{2} d_i^\top \nabla_S^2 f(x^0; D) d_i \\ &= f(x^0) + 2f(x^0 + d_i) - 2f(x^0) - \frac{1}{2} f(x^0 + 2d_i) + \frac{1}{2} f(x^0) + \frac{1}{2} (f(x^0 + 2d_i) - 2f(x^0 + d_i) + f(x^0)) \\ &= f(x^0 + d_i). \end{aligned} \quad (4)$$

Case III: Suppose $x = x^0 + d_i + d_j$ where $i, j \in \{1, \dots, p\}$. Notice that for all $i, j \in \{1, \dots, p\}$, the ij -th element of $\delta_{\delta_f(x^0; D)}$ is

$$f(x^0 + d_i + d_j) - f(x^0 + d_i) - f(x^0 + d_j) + f(x^0).$$

Using (4), and noticing that $\nabla_S^2 f(x^0; D)$ is symmetric ([23, Proposition 4.4]), we have

$$\begin{aligned}
& m(x^0 + d_i + d_j) \\
&= f(x^0) + (2\nabla_S f(x^0; D) - \nabla_S f(x^0; 2D))^\top (d_i + d_j) + \frac{1}{2} (d_i + d_j)^\top \nabla_S^2 f(x^0; D) (d_i + d_j) \\
&= m(x^0 + d_i) + m(x^0 + d_j) + d_i^\top \nabla_S^2 f(x^0; D) d_j - f(x^0) \\
&= f(x^0 + d_i) + f(x^0 + d_j) + f(x^0 + d_i + d_j) - f(x^0 + d_i) - f(x^0 + d_j) \\
&= f(x^0 + d_i + d_j).
\end{aligned}$$

□

Notice that all the sample points needed to construct the model $m(x)$ are contained in the affine space $\mathcal{Y} = \{x^0 + D\hat{s} : \hat{s} \in \mathbb{R}^p\}$. Hence, we can construct a model that interpolates f on the image of the points in \mathbb{R}^p . Recall that the QR -factorization of a matrix with full-column rank gives an orthonormal basis for its range, determined by Q , and the coordinates of its columns under this basis, determined by R . A determined quadratic model can be constructed in the subspace determined by R .

Definition 5 Given $D \in \mathbb{R}^{n \times p}$ with full-column rank, $f : \mathbb{R}^n \rightarrow \mathbb{R}$, and $x^0 \in \mathbb{R}^n$. Suppose the QR -factorization of D is $D = QR$, where $Q \in \mathbb{R}^{n \times p}$ and $R = [r_1 \cdots r_p] \in \mathbb{R}^{p \times p}$. Let $\hat{f}(\hat{s}) = f(x^0 + Q\hat{s})$. The model $\hat{m} : \mathbb{R}^p \rightarrow \mathbb{R}$ is defined by

$$\hat{m}(\hat{s}) = \hat{f}(\mathbf{0}) + \left(2\nabla_S \hat{f}(\mathbf{0}; R) - \nabla_S \hat{f}(\mathbf{0}; 2R)\right)^\top \hat{s} + \frac{1}{2} \hat{s}^\top \nabla_S^2 \hat{f}(\mathbf{0}; R) \hat{s}.$$

Theorem 2 The model $\hat{m}(\hat{s})$ is a determined quadratic interpolation model of \hat{f} in \mathbb{R}^p . In particular, $\hat{m}(\hat{s})$ interpolates $\hat{f}(\hat{s})$ on all sample points in

$$\hat{Y} = \{\mathbf{0}\} \cup \{r_i : i = 1, \dots, p\} \cup \{r_i + r_j : i, j = 1, \dots, p\}.$$

Proof Since D has full-column rank, we have that R is invertible and the $(p+1)(p+2)/2$ points in the set \hat{Y} are distinct. Therefore, we only need to show that $\hat{m}(\hat{s}) = \hat{f}(\hat{s})$ for all \hat{s} in the set \hat{Y} . The rest of the proof is analogous to the proof of Theorem 1. □

Remark 1 We note that the term

$$2\nabla_S \hat{f}(\mathbf{0}; R) - \nabla_S \hat{f}(\mathbf{0}; 2R)$$

in $\hat{m}(\hat{s})$ is the adapted centred simplex gradient [8] of \hat{f} over $\mathbb{Y} = \mathbb{Y}^+ \cup \tilde{\mathbb{Y}}$, where $\mathbb{Y}^+ = \{\mathbf{0}\} \cup \{r_i : i = 1, \dots, p\}$ and $\tilde{\mathbb{Y}} = \{\mathbf{0}\} \cup \{2r_i : i = 1, \dots, p\}$. Detailed explanations of the notation and more properties of the adapted centred simplex gradient can be found in [8].

As we noted at the beginning of this subsection, the underdetermined model in \mathbb{R}^n and the determined model in \mathbb{R}^p are equivalent. The following theorem shows how to convert between them.

Theorem 3 Suppose matrix $D = [d_1 \cdots d_p] \in \mathbb{R}^{n \times p}$ has full-column rank and let $x^0 \in \mathbb{R}^n$. Suppose the QR -factorization of D is $D = QR$, where $Q \in \mathbb{R}^{n \times p}$ and $R = [r_1 \cdots r_p] \in \mathbb{R}^{p \times p}$. Let $\hat{f}(\hat{s}) = f(x^0 + Q\hat{s})$. Then $m(x)$ and $\hat{m}(\hat{s})$ have the following relation

$$\hat{m}(\hat{s}) = m(x^0 + Q\hat{s}). \quad (5)$$

Moreover, for all $x \in \mathcal{Y} = \{x^0 + D\hat{s} : \hat{s} \in \mathbb{R}^p\}$, we have

$$m(x) = \hat{m}(Q^\top(x - x^0)). \quad (6)$$

Proof Notice that $d_i = Qr_i$ for all $i \in \{1, \dots, p\}$, therefore we have

$$\begin{aligned} f(x^0 + d_i) - f(x^0) &= \widehat{f}(r_i) - \widehat{f}(\mathbf{0}), \\ f(x^0 + 2d_i) - f(x^0) &= \widehat{f}(2r_i) - \widehat{f}(\mathbf{0}), \\ f(x^0 + d_i + d_j) - f(x^0 + d_i) &= \widehat{f}(r_i + r_j) - \widehat{f}(r_i), \end{aligned}$$

for all $i, j \in \{1, \dots, p\}$. These imply that

$$\delta_f(x^0; D) = \delta_{\widehat{f}}(\mathbf{0}; R), \quad \delta_f(x^0; 2D) = \delta_{\widehat{f}}(\mathbf{0}; 2R), \quad \delta_f(x^0 + d_i; D) = \delta_{\widehat{f}}(r_i; R),$$

for all $i \in \{1, \dots, p\}$.

Since $D = QR$ has full-column rank, we have

$$D^\dagger = (D^\top D)^{-1} D^\top = (R^\top Q^\top QR)^{-1} R^\top Q^\top = (R^\top R)^{-1} R^\top Q^\top = R^{-1} Q^\top,$$

which gives $D^\dagger Q = R^{-1}$. Hence, we have

$$\begin{aligned} \nabla_S f(x^0; D)^\top Q &= \delta_f(x^0; D)^\top D^\dagger Q = \delta_{\widehat{f}}(\mathbf{0}; R)^\top R^{-1} = \nabla_S \widehat{f}(\mathbf{0}; R)^\top, \\ \nabla_S f(x^0; 2D)^\top Q &= \delta_f(x^0; 2D)^\top (2D)^\dagger Q = \delta_{\widehat{f}}(\mathbf{0}; 2R)^\top (2R)^{-1} = \nabla_S \widehat{f}(\mathbf{0}; 2R)^\top, \\ \nabla_S f(x^0 + d_i; D)^\top Q &= \delta_f(x^0 + d_i; D)^\top D^\dagger Q = \delta_{\widehat{f}}(r_i; R)^\top R^{-1} = \nabla_S \widehat{f}(r_i; R)^\top, \end{aligned}$$

for all $i \in \{1, \dots, p\}$.

Based on these, we also have

$$\delta_{\nabla_S f}(x^0; D)Q = \begin{bmatrix} \left(\nabla_S \widehat{f}(r_1; R) - \nabla_S \widehat{f}(\mathbf{0}; R) \right)^\top \\ \left(\nabla_S \widehat{f}(r_2; R) - \nabla_S \widehat{f}(\mathbf{0}; R) \right)^\top \\ \vdots \\ \left(\nabla_S \widehat{f}(r_p; R) - \nabla_S \widehat{f}(\mathbf{0}; R) \right)^\top \end{bmatrix} = \delta_{\nabla_S \widehat{f}}(\mathbf{0}; R).$$

Therefore,

$$Q^\top \nabla_S^2 f(x^0; D)Q = (D^\dagger Q)^\top \delta_{\nabla_S f}(x^0; D)Q = \nabla_S^2 \widehat{f}(\mathbf{0}; R).$$

Let $x = x^0 + Q\widehat{s}$. Examining $m(x)$, we obtain

$$\begin{aligned} m(x) &= m(x^0 + Q\widehat{s}) \\ &= f(x^0) + \left(2\nabla_S f(x^0; D) - \nabla_S f(x^0; 2D) \right)^\top Q\widehat{s} + \frac{1}{2} \widehat{s}^\top Q^\top \nabla_S^2 f(x^0; D)Q\widehat{s} \\ &= \widehat{f}(\mathbf{0}) + \left(2\nabla_S \widehat{f}(\mathbf{0}; R) - \nabla_S \widehat{f}(\mathbf{0}; 2R) \right)^\top \widehat{s} + \frac{1}{2} \widehat{s}^\top \nabla_S^2 \widehat{f}(\mathbf{0}; R)\widehat{s} \\ &= \widehat{m}(\widehat{s}), \end{aligned}$$

which gives the relation in Equation (5).

For the second relation, notice that for all $x \in \mathcal{Y}$, there exists $\widehat{s} \in \mathbb{R}^p$ such that $x = x^0 + Q\widehat{s}$, or equivalently, $\widehat{s} = Q^\top(x - x^0)$. The second relation (6) follows from applying this change of notation to relation (5).

□

2.2 Complete algorithm

In this subsection, we give the complete QARSTA algorithm which consists of the main algorithm and three subroutines.

Algorithm 1: Main algorithm

| | | | |
|---------------|------------------------------------------------|-----------------------------------------------------------|------------------------------------------------|
| | f | $f : \mathbb{R}^n \rightarrow \mathbb{R}$ | objective function |
| | p_{rand}, p | $1 \leq p_{\text{rand}} \leq p \leq n$ | minimum randomized and full subspace dimension |
| | x_0, Δ_0 | $x_0 \in \mathbb{R}^n, \Delta_0 > 0$ | starting point and initial trust-region radius |
| | $\Delta_{\min}, \Delta_{\max}$ | $0 < \Delta_{\min} \leq \Delta_{\max}$ | minimum and maximum trust-region radii |
| Input: | $\gamma_{\text{dec}}, \gamma_{\text{inc}}$ | $0 < \gamma_{\text{dec}} < 1 < \gamma_{\text{inc}}$ | trust-region radius updating parameters |
| | η_1, η_2 | $0 < \eta_1 \leq \eta_2 < 1$ | acceptance thresholds |
| | μ | $\mu > 0$ | criticality constant |
| | $\epsilon_{\text{rad}}, \epsilon_{\text{geo}}$ | $\epsilon_{\text{rad}} \geq 1, \epsilon_{\text{geo}} > 0$ | sample set radius and geometry tolerance |
| | M_A | $M_A \geq 1$ | normal distribution matrix upper bound |

Initialize: Generate random mutually orthogonal directions $d_1, \dots, d_p \in \mathbb{R}^n$ with length Δ_0 by Algorithm 4; define initial direction matrix $D_0 = [d_1 \cdots d_p]$.

for $k = 0, 1, \dots$ **do**

Perform the QR -factorization $D_k = Q_k R_k$ and construct model \hat{m}_k at x_k .

if $\mu \|\nabla \hat{m}_k(\mathbf{0})\| < \Delta_k$ // Criticality test

Set $\Delta_{k+1} = \gamma_{\text{dec}} \Delta_k, x_{k+1} = x_k$ and $D_{k+1} = \gamma_{\text{dec}} D_k$.

else // Trust-region subproblem and update

Solve (approximately)

$$\min_{\hat{s}_k \in \mathbb{R}^p} \hat{m}_k(\hat{s}_k) \quad \text{s.t.} \quad \|\hat{s}_k\| \leq \Delta_k$$

and calculate the step $s_k = Q_k \hat{s}_k \in \mathbb{R}^n$.

Calculate

$$\rho_k = \frac{f(x_k) - f(x_k + s_k)}{\hat{m}_k(\mathbf{0}) - \hat{m}_k(\hat{s}_k)}$$

and update the trust-region radius

$$\Delta_{k+1} = \begin{cases} \gamma_{\text{dec}} \Delta_k, & \text{if } \rho_k < \eta_1, \\ \min(\gamma_{\text{inc}} \Delta_k, \Delta_{\max}), & \text{if } \rho_k > \eta_2 \text{ and } \|\hat{s}_k\| \geq 0.95 \Delta_k, \\ \Delta_k, & \text{otherwise.} \end{cases}$$

Let x_{k+1} be any point such that

$$f(x_{k+1}) \leq \min \{ \{f(x_k + s_k)\} \cup \{f(x_k + d_i + d_j) : d_i, d_j \in [\mathbf{0} D_k]\} \}. \quad (7)$$

Create D_{k+1}^U according to Algorithm 2 and denote the columns of D_{k+1}^U by $d_1^U, \dots, d_{p_1}^U$ where $0 \leq p_1 \leq p$.

Generate $q = p - p_1$ random mutually orthogonal directions d_1^R, \dots, d_q^R with length Δ_{k+1} that are orthogonal to all columns in D_{k+1}^U using Algorithm 4.

Set $D_{k+1} = [d_1^U \cdots d_{p_1}^U \ d_1^R \cdots d_q^R]$.

end

if $\Delta_{k+1} < \Delta_{\min}$, **stop.** // Stopping test

end

Algorithm 2: Creating D_{k+1}^U algorithm

Input: $D_k; x_k; x_{k+1}; s_k; \Delta_{k+1}; p; p_{\text{rand}}; \epsilon_{\text{rad}}; \epsilon_{\text{geo}}$.
 Select p directions from $\{\{x_k + s_k - x_{k+1}\} \cup \{x_k + d_i + d_j - x_{k+1} : d_i, d_j \in [\mathbf{0} \ D_k]\}\}$ as the columns of D_{k+1}^U .
 Remove p_{rand} directions from D_{k+1}^U using Algorithm 3.
 Remove all directions $d \in D_{k+1}^U$ with $\|d\| > \epsilon_{\text{rad}} \Delta_{k+1}$.
while D_{k+1}^U is not empty and $\sigma_{\min}(D_{k+1}^U) < \epsilon_{\text{geo}}$ **do**
 | Remove 1 direction from D_{k+1}^U using Algorithm 3.
end

Algorithm 3: Direction removing algorithm

Input: $D_{k+1}^U; \Delta_{k+1}$; number of directions to be removed p_{rm} .
 Set the number of directions removed **removed** = 0.
while **removed** < p_{rm} **do**
 | Denote $D_{k+1}^U = [d_1^U \cdots d_m^U]$.
 | **for** $i = 1, \dots, m$ **do**
 | | Define matrix $M_i = [d_1^U \cdots d_{i-1}^U \ d_{i+1}^U \cdots d_m^U]$ and compute
 | |
$$\theta_i = \sigma_{\min}(M_i) \cdot \max\left(\frac{\|d_i^U\|^4}{\Delta_{k+1}^4}, 1\right).$$

 | | **end**
 | Remove the direction with the largest θ_i from D_{k+1}^U , set **removed** = **removed** + 1.
end

Algorithm 4: Direction generating algorithm (modified from [6, Algorithm 5])

Input: Orthonormal basis for current subspace Q (optional); number of new directions q ; length of new directions Δ ; M_A .
 Generate $A \in \mathbb{R}^{n \times q}$ with $A_{ij} \sim \mathcal{N}(0, 1/q)$ such that A has full-column rank and $\|A\| \leq M_A$.
 If Q is specified, then calculate $\tilde{A} = A - QQ^\top A$, otherwise set $\tilde{A} = A$.
 Perform the QR -factorization $\tilde{A} = \tilde{Q}\tilde{R}$ and denote $\tilde{Q} = [\tilde{q}_1 \cdots \tilde{q}_q]$.
 Return $\Delta_{\tilde{q}_1}, \dots, \Delta_{\tilde{q}_q}$.

We note that the trust-region subproblem is solved approximately by an implementation in [6] of the routine TRSBOX from BOBYQA [33]. The way we set the next iterate (inequality (7)) gives some flexibility to QARSTA by allowing it to use other optimization algorithms (e.g., heuristics) to improve efficiency without breaking convergence. We also note that, unlike some other model-based trust-region algorithms (e.g., [4, Algorithm 11.1]), the stopping condition of QARSTA does not check if the model gradient is small enough. This is because, in QARSTA, a small model gradient implies a small true gradient only if the current subspace has a certain good quality. As we will explain in Subsection 2.5, the subspaces in QARSTA have this good quality with a certain probability and therefore model gradients do not always provide sufficient information on true gradients.

2.3 Sample set geometry

In this subsection, we examine the sample set management procedure in QARSTA (Algorithms 2 to 4).

In each iteration of QARSTA, we replace at least p_{rand} directions to construct the next direction matrix. Our criteria for dropping and adding directions are based on the idea that $\|D_k^\dagger\|$ should be as small as possible. We will see in Subsection 2.4 (Theorem 6) that $\|D_k^\dagger\|$ is directly related to error bounds and minimizing it improves our bounds on model accuracy.

Our management procedure is such that $\|D_k^\dagger\| = 1/\sigma_{\min}(D_k)$ is minimized, i.e., $\sigma_{\min}(D_k)$ is maximized. The following theorem shows the relation between $\sigma_{\min}(D_k)$ and the columns of D_k .

Theorem 4 *Let $\tilde{D} = [d_1 \cdots d_{q-1}] \in \mathbb{R}^{n \times (q-1)}$ where $2 \leq q \leq n$. Define $D(x) : \mathbb{R}^n \rightarrow \mathbb{R}^{n \times q}$ by $D(x) = [\tilde{D} \ x]$. Let $\Delta > 0$. Then for all $x \in \mathbb{R}^n$ with $\|x\| = \Delta$, we have*

$$\sigma_{\min}(D(x)) \leq \min \left\{ \sigma_{\min}(\tilde{D}), \Delta \right\}.$$

In particular, if $x^ \in \mathbb{R}^n$ with $\|x^*\| = \Delta$ satisfies $d_i^\top x^* = 0$ for all $i \in \{1, \dots, q-1\}$, then*

$$\sigma_{\min}(D(x^*)) = \min \left\{ \sigma_{\min}(\tilde{D}), \Delta \right\}.$$

Proof Let $x \in \mathbb{R}^n$ such that $\|x\| = \Delta$. Since $q \leq n$, we have $\sigma_{\min}(D(x)) = \min_{\|y\|=1} \|D(x)y\|$ ([25, Theorem 3.1.2]). Consider $y = [y_1, \dots, y_q]^\top \in \mathbb{R}^q$. Since $q \geq 2$, we can let $y_q = 0$ and obtain

$$\min_{\|y\|=1} \|D(x)y\| \leq \min_{\|y\|=1, y_q=0} \|D(x)y\| = \min_{\|w\|=1} \|\tilde{D}w\| = \sigma_{\min}(\tilde{D}).$$

Clearly,

$$\min_{\|y\|=1} \|D(x)y\| \leq \left\| D(x)e_q^{(q)} \right\| = \|x\| = \Delta.$$

Therefore, we have

$$\sigma_{\min}(D(x)) \leq \min \left\{ \sigma_{\min}(\tilde{D}), \Delta \right\},$$

which gives the first inequality.

Now we prove the second equality. Recall that $\sigma_{\min}(M) = \sqrt{\lambda_{\min}(M^\top M)}$ for any matrix $M \in \mathbb{R}^{n \times z}$ with $z \leq n$. Since $d_i^\top x^* = 0$ for all $i \in \{1, \dots, q-1\}$, we have $\tilde{D}^\top x^* = \mathbf{0}$. Hence,

$$D(x^*)^\top D(x^*) = \begin{bmatrix} \tilde{D}^\top \tilde{D} & \mathbf{0}^\top \\ \mathbf{0} & (x^*)^\top x^* \end{bmatrix},$$

whose eigenvalues are all eigenvalues of $\tilde{D}^\top \tilde{D}$ and $(x^*)^\top x^* = \Delta^2$. Therefore, we obtain

$$\sigma_{\min}(D(x^*)) = \sqrt{\min \left\{ \lambda_{\min}(\tilde{D}^\top \tilde{D}), \Delta^2 \right\}} = \min \left\{ \sigma_{\min}(\tilde{D}), \Delta \right\},$$

which gives the second equality. □

Theorem 4 shows that if we want to add a column to a matrix using a vector with magnitude Δ such that the minimum singular value of the new matrix is maximized, then the best choice is a vector orthogonal to all the current columns. This gives us the criterion for adding new directions, which is applied in Algorithm 4.

Notice that Theorem 4 also says that the largest possible minimum singular value of the new matrix is the minimum of the current minimum singular value and Δ . This implies that the subspaces constructed using Algorithms 2 to 4 satisfy

$$\|D_k^\dagger\| = \begin{cases} 1/\Delta_k, & D_k^U \text{ is empty,} \\ \max\{1/\sigma_{\min}(D_k^U), 1/\Delta_k\}, & D_k^U \text{ is not empty,} \end{cases}$$

where the first case comes from the fact that when D_k^U is empty, D_k consists of mutually orthogonal columns with length Δ_k . Since Algorithm 2 guarantees that $\sigma_{\min}(D_k^U) \geq \epsilon_{\text{geo}}$ whenever D_k^U is not empty, we always have

$$\|D_k^\dagger\| \leq \max\left\{\frac{1}{\epsilon_{\text{geo}}}, \frac{1}{\Delta_{\min}}\right\}, \quad (8)$$

Inequality (8) is an important property and we will return to it later in Subsection 2.4.

This also implies a criterion for removing directions. That is, we want to drop the direction such that the remaining matrix has the largest minimum singular value. This criterion is applied in Algorithm 3.

We note that Algorithm 3 is different from the procedure used in [6], which calculates the vector of θ_i values once and simultaneously removes directions with the largest θ_i . The following example shows that these two procedures may produce different results.

Example 1 Suppose $\Delta_{k+1} = 1$. Suppose we want to drop two directions from

$$D_{k+1}^U = \begin{bmatrix} \frac{1}{2\sqrt{3}} & \frac{1}{\sqrt{3}} & \frac{1}{\sqrt{3}} \\ 0 & \frac{1}{\sqrt{3}} & \frac{1}{\sqrt{3}} \\ 0 & \frac{1}{\sqrt{3}} & \frac{1}{2\sqrt{3}} \end{bmatrix}.$$

Then we have

$$M_1 = \begin{bmatrix} \frac{1}{\sqrt{3}} & \frac{1}{\sqrt{3}} \\ \frac{1}{\sqrt{3}} & \frac{1}{\sqrt{3}} \\ \frac{1}{\sqrt{3}} & \frac{1}{2\sqrt{3}} \end{bmatrix}, \quad M_2 = \begin{bmatrix} \frac{1}{2\sqrt{3}} & \frac{1}{\sqrt{3}} \\ 0 & \frac{1}{\sqrt{3}} \\ 0 & \frac{1}{2\sqrt{3}} \end{bmatrix}, \quad M_3 = \begin{bmatrix} \frac{1}{2\sqrt{3}} & \frac{1}{\sqrt{3}} \\ 0 & \frac{1}{\sqrt{3}} \\ 0 & \frac{1}{\sqrt{3}} \end{bmatrix},$$

with minimum singular values

$$\sigma_{\min}(M_1) \approx 0.180, \quad \sigma_{\min}(M_2) \approx 0.210, \quad \sigma_{\min}(M_3) \approx 0.232.$$

Hence, we have

$$\begin{aligned} \theta_1 &\approx 0.180 \cdot \max\left\{\left(\frac{1}{2\sqrt{3}}\right)^4, 1\right\} = 0.180, \\ \theta_2 &\approx 0.210 \cdot \max\{1^4, 1\} = 0.210, \\ \theta_3 &\approx 0.232 \cdot \max\left\{\left(\frac{3}{4}\right)^4, 1\right\} = 0.232. \end{aligned}$$

According to the procedure used in [6], we would drop the last two directions $[1/\sqrt{3}, 1/\sqrt{3}, 1/\sqrt{3}]^\top$, $[1/\sqrt{3}, 1/\sqrt{3}, 1/2\sqrt{3}]^\top$. The minimum singular value of the remaining matrix is $\sigma_{\min}([1/2\sqrt{3}, 0, 0]^\top) \approx 0.289$.

However, if we use Algorithm 3, then we drop the last direction $[1/\sqrt{3}, 1/\sqrt{3}, 1/2\sqrt{3}]^\top$ and update

$$M_1 = \begin{bmatrix} \frac{1}{\sqrt{3}} \\ \frac{1}{\sqrt{3}} \\ \frac{1}{\sqrt{3}} \end{bmatrix}, \quad M_2 = \begin{bmatrix} \frac{1}{2\sqrt{3}} \\ 0 \\ 0 \end{bmatrix},$$

which gives

$$\theta_1 = 1, \quad \theta_2 \approx 0.289.$$

Next, we drop the first direction $[1/2\sqrt{3}, 0, 0]^\top$ and the minimum singular value of the remaining matrix is $\sigma_{\min}([1/\sqrt{3}, 1/\sqrt{3}, 1/\sqrt{3}]^\top) = 1$.

Since $1 > 0.289$, in Example 1, the result given by Algorithm 3 is better than the procedure used in [6]. In fact, if $p_{\text{rm}} \leq 2$, then the result given by Algorithm 3 is always no worse than the procedure used in [6]. Indeed, the first direction removed by both procedures is always the same. For the second direction, Algorithm 3 calculates the θ_i of every remaining direction, including the second direction removed by the procedure used in [6], and removes the direction with the largest value. However, if $p_{\text{rm}} > 2$, then we do not have guarantees on which procedure gives the better result. In fact, we have randomly generated matrices $D_{k+1}^U \in \mathbb{R}^{4 \times 4}$ and let $p_{\text{rm}} = 3$. Numerical results of running each procedure on these matrices show that there are cases in which each of the procedures produces better results. Future research could further explore this problem and develop an optimal strategy for removing directions.

2.4 Model accuracy

In QARSTA, we require the models to provide a certain level of accuracy in the subspaces. Hence, following [6], we introduce the notion of Q -fully linear models and Q -fully quadratic models.

Definition 6 Given $f \in \mathcal{C}^1$, $x \in \mathbb{R}^n$, $\bar{\Delta} > 0$, and $Q \in \mathbb{R}^{n \times p}$, we say that $\mathcal{M}_{\bar{\Delta}} = \{\hat{m}_{\Delta} : \mathbb{R}^p \rightarrow \mathbb{R}\}_{\Delta \in (0, \bar{\Delta}]}$ is a class of Q -fully linear models of f at x parameterized by Δ if there exists constants $\kappa_{ef}(x) > 0$ and $\kappa_{eg}(x) > 0$ such that for all $\Delta \in (0, \bar{\Delta}]$ and $\hat{s} \in \mathbb{R}^p$ with $\|\hat{s}\| \leq \Delta$,

$$\begin{aligned} |f(x + Q\hat{s}) - \hat{m}_{\Delta}(\hat{s})| &\leq \kappa_{ef}(x)\Delta^2, \\ \|Q^\top \nabla f(x + Q\hat{s}) - \nabla \hat{m}_{\Delta}(\hat{s})\| &\leq \kappa_{eg}(x)\Delta. \end{aligned}$$

Definition 7 Given $f \in \mathcal{C}^2$, $x \in \mathbb{R}^n$, $\bar{\Delta} > 0$, and $Q \in \mathbb{R}^{n \times p}$, we say that $\mathcal{M}_{\bar{\Delta}} = \{\hat{m}_{\Delta} : \mathbb{R}^p \rightarrow \mathbb{R}\}_{\Delta \in (0, \bar{\Delta}]}$ is a class of Q -fully quadratic models of f at x parameterized by Δ if there exists constants $\kappa_{ef}(x) > 0$, $\kappa_{eg}(x) > 0$, and $\kappa_{eh}(x) > 0$ such that for all $\Delta \in (0, \bar{\Delta}]$ and $\hat{s} \in \mathbb{R}^p$ with $\|\hat{s}\| \leq \Delta$,

$$\begin{aligned} |f(x + Q\hat{s}) - \hat{m}_{\Delta}(\hat{s})| &\leq \kappa_{ef}(x)\Delta^3, \\ \|Q^\top \nabla f(x + Q\hat{s}) - \nabla \hat{m}_{\Delta}(\hat{s})\| &\leq \kappa_{eg}(x)\Delta^2, \\ \|Q^\top \nabla^2 f(x + Q\hat{s})Q - \nabla^2 \hat{m}_{\Delta}(\hat{s})\| &\leq \kappa_{eh}(x)\Delta. \end{aligned}$$

Clearly, if $\mathcal{M}_{\bar{\Delta}}$ is a class of Q -fully quadratic models of f at x , then $\mathcal{M}_{\bar{\Delta}}$ is also a class of Q -fully linear models of f at x .

In this subsection, we develop error bounds for the models and show that each \hat{m}_k belongs to a class of Q_k -fully quadratic models of f at x_k , where $Q_k R_k$ is the QR -factorization of D_k . Moreover, we show that constants κ_{ef} , κ_{eg} , and κ_{eh} are independent of k .

We note that the convergence of QARSTA only requires that each \hat{m}_k belongs to a class of Q_k -fully linear models (see Section 3 for details). As this requirement is weaker than Q_k -fully quadratic, our convergence analysis holds for \hat{m}_k .

We begin by introducing two lemmas that are crucial to the proof of the error bounds. The first lemma is an application of Taylor's theorem.

Lemma 1 *Let $x \in \mathbb{R}^n$, $\Delta > 0$, and $f \in \mathcal{C}^{2+}$ on $B(x; \Delta)$ with constant $L_{\nabla^2 f}$. For all $d \in \mathbb{R}^n$ with $\|d\| \leq \Delta$,*

$$\left| f(x+d) - f(x) - \nabla f(x)^\top d - \frac{1}{2} d^\top \nabla^2 f(x) d \right| \leq \frac{1}{6} L_{\nabla^2 f} \|d\|^3.$$

Proof See [14, Lemma 4.1.14]. □

The second lemma is an error bound for the generalized simplex Hessian. This result is a simple extension of the error bound presented in [23].

Lemma 2 *Let $x^0 \in \mathbb{R}^n$, $\bar{\Delta} > 0$, and $f \in \mathcal{C}^{2+}$ on $B(x^0; \bar{\Delta})$ with constant $L_{\nabla^2 f}$. Suppose $D = [d_1 \cdots d_n] \in \mathbb{R}^{n \times n}$ is invertible and $\overline{\text{diam}}(D) = \max_{1 \leq i \leq n} \|d_i\| \leq \bar{\Delta}$. Then for all $x \in B(x^0; \overline{\text{diam}}(D))$ we have*

$$\|\nabla^2 f(x) - \nabla_S^2 f(x^0; D)\| \leq 4nL_{\nabla^2 f} \left\| \widehat{D}^{-\top} \right\|^2 \overline{\text{diam}}(D) + L_{\nabla^2 f} \overline{\text{diam}}(D),$$

where $\widehat{D} = D/\overline{\text{diam}}(D)$.

Proof Using Lemma 1, the proof of [23, Theorem 4.2] holds for $f \in \mathcal{C}^{2+}$, we see that

$$\|\nabla^2 f(x^0) - \nabla_S^2 f(x^0; D)\| \leq 4nL_{\nabla^2 f} \left\| \widehat{D}^{-\top} \right\|^2 \overline{\text{diam}}(D).$$

The proof is complete by noticing that

$$\|\nabla^2 f(x) - \nabla_S^2 f(x^0; D)\| \leq \|\nabla^2 f(x^0) - \nabla_S^2 f(x^0; D)\| + \|\nabla^2 f(x) - \nabla^2 f(x^0)\|$$

and

$$\|\nabla^2 f(x) - \nabla^2 f(x^0)\| \leq L_{\nabla^2 f} \|x - x^0\| \leq L_{\nabla^2 f} \overline{\text{diam}}(D).$$

□

Now we can start to develop the error bounds for \hat{m} . The next lemma shows that restricting f to a subspace determined by an orthonormal basis does not increase its Lipschitz constant.

Lemma 3 *Suppose $f \in \mathcal{C}^{2+}$ with Lipschitz constant $L_{\nabla^2 f}$. Suppose $Q \in \mathbb{R}^{n \times p}$ consists of p orthonormal columns and let $x \in \mathbb{R}^n$. Let $\hat{f}(\hat{s}) = f(x + Q\hat{s})$. Then $\nabla^2 \hat{f}$ is Lipschitz continuous on \mathbb{R}^p with constant $L_{\nabla^2 f}$.*

Henceforth, we will not differentiate between the Lipschitz constant of $\nabla^2 f$ on \mathbb{R}^n and $\nabla^2 \hat{f}$ on \mathbb{R}^p , and denote them both by $L_{\nabla^2 f}$.

The following theorem gives the error bounds for \hat{m} . The bounds are given in terms of matrix R , but in Theorem 6 we shall explain how the error bounds are related to $\|D_k^\dagger\|$, which is controlled by our sample set management procedure (see Subsection 2.3 for details).

In the following results, we suppose $R = [r_1 \cdots r_p]$ and denote

$$\overline{\text{diam}}(R) = \max_{1 \leq i \leq p} \|r_i\| \quad \text{and} \quad \hat{R} = \frac{1}{\overline{\text{diam}}(R)} R.$$

The proof is inspired by [12, Theorem 3.16].

Theorem 5 *Suppose $f \in \mathcal{C}^{2+}$ with Lipschitz constant $L_{\nabla^2 f}$. Suppose $D \in \mathbb{R}^{n \times p}$ has full-column rank and let $x^0 \in \mathbb{R}^n$. Suppose the QR-factorization of D is $D = QR$, where $Q \in \mathbb{R}^{n \times p}$ and $R \in \mathbb{R}^{p \times p}$. Let $\hat{f}(\hat{s}) = f(x^0 + Q\hat{s})$. Then for all $\hat{s} \in \mathbb{R}^p$ with $\|\hat{s}\| \leq \overline{\text{diam}}(R)$, we have*

$$\|Q^\top \nabla^2 f(x^0 + Q\hat{s})Q - \nabla^2 \hat{m}(\hat{s})\| \leq L_{\nabla^2 f} \left(4p \|\hat{R}^{-\top}\|^2 + 1 \right) \overline{\text{diam}}(R),$$

$$\|Q^\top \nabla f(x^0 + Q\hat{s}) - \nabla \hat{m}(\hat{s})\| \leq 3\sqrt{p}L_{\nabla^2 f} \|\hat{R}^{-\top}\| \left(2p \|\hat{R}^{-\top}\|^2 + 1 \right) \overline{\text{diam}}(R)^2,$$

and

$$\begin{aligned} & |f(x^0 + Q\hat{s}) - \hat{m}(\hat{s})| \\ & \leq \left(\sqrt{p}L_{\nabla^2 f} \|\hat{R}^{-\top}\| \left(6p \|\hat{R}^{-\top}\|^2 + 2\sqrt{p} \|\hat{R}^{-\top}\| + 3 \right) + \frac{2}{3}L_{\nabla^2 f} \right) \overline{\text{diam}}(R)^3. \end{aligned}$$

Proof For simplicity, we denote

$$\hat{m}(\hat{s}) = c + \hat{g}^\top \hat{s} + \frac{1}{2} \hat{s}^\top \hat{H} \hat{s} \quad (9)$$

and define the error between the model and true values by

$$E^f(\hat{s}) = \hat{m}(\hat{s}) - \hat{f}(\hat{s}), \quad (10)$$

$$E^g(\hat{s}) = \nabla \hat{m}(\hat{s}) - \nabla \hat{f}(\hat{s}) = \hat{g} + \hat{H} \hat{s} - \nabla \hat{f}(\hat{s}), \quad (11)$$

$$E^H(\hat{s}) = \nabla^2 \hat{m}(\hat{s}) - \nabla^2 \hat{f}(\hat{s}) = \hat{H} - \nabla^2 \hat{f}(\hat{s}). \quad (12)$$

According to Lemma 2, we have

$$\|E^H(\hat{s})\| = \|\hat{H} - \nabla^2 \hat{f}(\hat{s})\| \leq L_{\nabla^2 f} \left(4p \|\hat{R}^{-\top}\|^2 + 1 \right) \overline{\text{diam}}(R),$$

which is the first error bound.

Since \hat{m} interpolates \hat{f} on $\{\mathbf{0}\} \cup \{r_i : i = 1, \dots, p\}$ (Theorem 2), we have

$$\hat{m}(r_i) = c + \hat{g}^\top r_i + \frac{1}{2} r_i^\top \hat{H} r_i = \hat{f}(r_i)$$

for all $r_i \in [\mathbf{0} \ r_1 \cdots r_p]$. Subtracting (9) from this equation, and noticing that \hat{H} is symmetric ([23, Proposition 4.4]), we obtain

$$\hat{m}(r_i) - \hat{m}(\hat{s}) = (r_i - \hat{s})^\top \hat{g} + \frac{1}{2} (r_i - \hat{s})^\top \hat{H} (r_i - \hat{s}) + (r_i - \hat{s})^\top \hat{H} \hat{s} = \hat{f}(r_i) - \hat{m}(\hat{s}) \quad (13)$$

for all $r_i \in [\mathbf{0} \ r_1 \cdots r_p]$. Substituting the expression of $\widehat{m}(\widehat{s})$, \widehat{g} , and \widehat{H} from (10) to (12) into (13), then regrouping terms, we get

$$\begin{aligned} (r_i - \widehat{s})^\top E^g(\widehat{s}) + \frac{1}{2} (r_i - \widehat{s})^\top E^H(\widehat{s}) (r_i - \widehat{s}) &= \widehat{f}(r_i) - \widehat{f}(\widehat{s}) - (r_i - \widehat{s})^\top \nabla \widehat{f}(\widehat{s}) \\ &\quad - \frac{1}{2} (r_i - \widehat{s})^\top \nabla^2 \widehat{f}(\widehat{s}) (r_i - \widehat{s}) - E^f(\widehat{s}), \end{aligned} \quad (14)$$

for all $r_i \in [\mathbf{0} \ r_1 \cdots r_p]$. In particular, when $r_i = \mathbf{0}$, we have

$$-\widehat{s}^\top E^g(\widehat{s}) + \frac{1}{2} \widehat{s}^\top E^H(\widehat{s}) \widehat{s} = \widehat{f}(\mathbf{0}) - \widehat{f}(\widehat{s}) - (-\widehat{s})^\top \nabla \widehat{f}(\widehat{s}) - \frac{1}{2} (-\widehat{s})^\top \nabla^2 \widehat{f}(\widehat{s}) (-\widehat{s}) - E^f(\widehat{s}). \quad (15)$$

Since \widehat{H} and $\nabla^2 \widehat{f}(\widehat{s})$ are symmetric, we have $E^H(\widehat{s})$ is symmetric. Subtracting (15) from (14), then regrouping terms, we get

$$r_i^\top E^g(\widehat{s}) = r_i^\top E^H(\widehat{s}) \widehat{s} - \frac{1}{2} r_i^\top E^H(\widehat{s}) r_i + \text{Rem}_i - \text{Rem}_0 \quad (16)$$

for all $r_i \in [r_1 \cdots r_p]$, where

$$\text{Rem}_i = \widehat{f}(r_i) - \widehat{f}(\widehat{s}) - (r_i - \widehat{s})^\top \nabla \widehat{f}(\widehat{s}) - \frac{1}{2} (r_i - \widehat{s})^\top \nabla^2 \widehat{f}(\widehat{s}) (r_i - \widehat{s})$$

and

$$\text{Rem}_0 = \widehat{f}(\mathbf{0}) - \widehat{f}(\widehat{s}) - (-\widehat{s})^\top \nabla \widehat{f}(\widehat{s}) - \frac{1}{2} (-\widehat{s})^\top \nabla^2 \widehat{f}(\widehat{s}) (-\widehat{s}).$$

According to Lemma 1, the above two terms have upper bounds

$$|\text{Rem}_i| \leq \frac{1}{6} L_{\nabla^2 f} \|r_i - \widehat{s}\|^3 \quad \text{and} \quad |\text{Rem}_0| \leq \frac{1}{6} L_{\nabla^2 f} \|-\widehat{s}\|^3.$$

Notice that $\|r_i - \widehat{s}\| \leq 2\overline{\text{diam}}(R)$, so (16) gives

$$\begin{aligned} |r_i^\top E^g(\widehat{s})| &= \left| r_i^\top E^H(\widehat{s}) \widehat{s} - \frac{1}{2} r_i^\top E^H(\widehat{s}) r_i + \text{Rem}_i - \text{Rem}_0 \right| \\ &\leq \|E^H(\widehat{s})\| \|\widehat{s}\| \|r_i\| + \frac{1}{2} \|E^H(\widehat{s})\| \|r_i\|^2 + |\text{Rem}_i| + |\text{Rem}_0| \\ &\leq \left(\|E^H(\widehat{s})\| + \frac{1}{2} \|E^H(\widehat{s})\| \right) \overline{\text{diam}}(R)^2 + \frac{1}{6} L_{\nabla^2 f} \|r_i - \widehat{s}\|^3 + \frac{1}{6} L_{\nabla^2 f} \|-\widehat{s}\|^3 \\ &\leq L_{\nabla^2 f} \left(6p \|\widehat{R}^{-\top}\|^2 + \frac{3}{2} \right) \overline{\text{diam}}(R)^3 + \frac{1}{6} L_{\nabla^2 f} (8\overline{\text{diam}}(R)^3 + \overline{\text{diam}}(R)^3) \\ &= 3L_{\nabla^2 f} \left(2p \|\widehat{R}^{-\top}\|^2 + 1 \right) \overline{\text{diam}}(R)^3, \end{aligned}$$

for all $r_i \in [r_1 \cdots r_p]$. Therefore, we obtain the second error bound

$$\begin{aligned} \|Q^\top \nabla f(x^0 + Q\widehat{s}) - \nabla \widehat{m}(\widehat{s})\| &= \|E^g(\widehat{s})\| \\ &= \|\widehat{R}^{-\top} \widehat{R}^\top E^g(\widehat{s})\| \\ &\leq \|\widehat{R}^{-\top}\| \|\widehat{R}^\top E^g(\widehat{s})\| \\ &= \|\widehat{R}^{-\top}\| \frac{1}{\overline{\text{diam}}(R)} \sqrt{\sum_{i=1}^p |r_i^\top E^g(\widehat{s})|^2} \end{aligned}$$

$$\leq 3\sqrt{p}L_{\nabla^2 f} \left\| \widehat{R}^{-\top} \right\| \left(2p \left\| \widehat{R}^{-\top} \right\|^2 + 1 \right) \overline{\text{diam}}(R)^2.$$

For the third error bound, we regroup (15) to get

$$E^f(\widehat{s}) = \text{Rem}_0 + \widehat{s}^\top E^g(\widehat{s}) - \frac{1}{2} \widehat{s}^\top E^H(\widehat{s}) \widehat{s}.$$

Applying the error bounds for $\|E^g(\widehat{s})\|$ and $\|E^H(\widehat{s})\|$, we obtain

$$\begin{aligned} |E^f(\widehat{s})| &\leq |\text{Rem}_0| + \|E^g(\widehat{s})\| \|\widehat{s}\| + \frac{1}{2} \|E^H(\widehat{s})\| \|\widehat{s}\|^2 \\ &= \left(\sqrt{p}L_{\nabla^2 f} \left\| \widehat{R}^{-\top} \right\| \left(6p \left\| \widehat{R}^{-\top} \right\|^2 + 2\sqrt{p} \left\| \widehat{R}^{-\top} \right\| + 3 \right) + \frac{2}{3} L_{\nabla^2 f} \right) \overline{\text{diam}}(R)^3. \end{aligned}$$

□

Now we show that each \widehat{m}_k belongs to a class of Q_k -fully quadratic models of f at x_k parameterized by $\Delta_k \in (0, \Delta_{\max}]$ and the constants κ_{ef} , κ_{eg} , and κ_{eh} are independent of k . To do this, we need to find the relation between $\overline{\text{diam}}(R_k)$ and Δ_k , and show that the coefficients of Δ_k and Δ_k^2 in the new error bounds do not depend on k .

We first note that $D_k = [d_1 \cdots d_p] = Q_k R_k = [Q_k r_1 \cdots Q_k r_p]$, so

$$\overline{\text{diam}}(R_k) = \max_{1 \leq i \leq p} \|r_i\| = \max_{1 \leq i \leq p} \|Q_k r_i\| = \max_{1 \leq i \leq p} \|d_i\|.$$

Notice that D_k is constructed in the $(k-1)$ -st iteration using Algorithms 2 to 4. Hence, any directions with a length larger than $\frac{\epsilon_{\text{rad}}}{\Delta_k}$ are removed and all new directions have a length equal to Δ_k . Therefore, we have $\overline{\text{diam}}(R_k) \leq \epsilon_{\text{rad}} \Delta_k \leq \epsilon_{\text{rad}} \Delta_{\max}$. Since each direction matrix D_k in QARSTA contains at least one new direction created by Algorithm 4, we also have $\Delta_k \leq \overline{\text{diam}}(R_k)$.

Finally to prove the following theorem, we also need the result of Subsection 2.3 that $\|D_k^\dagger\| \leq \max\{1/\epsilon_{\text{geo}}, 1/\Delta_{\min}\}$ (inequality (8)).

Theorem 6 *Suppose $f \in \mathcal{C}^{2+}$ with Lipschitz constant $L_{\nabla^2 f}$. Suppose $D_k \in \mathbb{R}^{n \times p}$ has full-column rank and let $x_k \in \mathbb{R}^n$. Suppose the QR-factorization of D_k is $D_k = Q_k R_k$, where $Q_k \in \mathbb{R}^{n \times p}$ and $R_k \in \mathbb{R}^{p \times p}$. Let $\widehat{f}(\widehat{s}) = f(x_k + Q_k \widehat{s})$. Then \widehat{m}_k belongs to a class of Q_k -fully quadratic models of f at x_k parameterized by $\Delta_k \in (0, \Delta_{\max}]$ with the following constants (which do not depend on k)*

$$\begin{aligned} \kappa_{ef} &= \left(\sqrt{p}L_{\nabla^2 f} M_{\widehat{R}^{-\top}} \left(6pM_{\widehat{R}^{-\top}}^2 + 2\sqrt{p}M_{\widehat{R}^{-\top}} + 3 \right) + \frac{2}{3} L_{\nabla^2 f} \right) \epsilon_{\text{rad}}^3, \\ \kappa_{eg} &= 3\sqrt{p}L_{\nabla^2 f} M_{\widehat{R}^{-\top}} \left(2pM_{\widehat{R}^{-\top}}^2 + 1 \right) \epsilon_{\text{rad}}^2, \\ \kappa_{eh} &= L_{\nabla^2 f} \left(4pM_{\widehat{R}^{-\top}}^2 + 1 \right) \epsilon_{\text{rad}}, \end{aligned}$$

where $M_{\widehat{R}^{-\top}} = \max\{1/\epsilon_{\text{geo}}, 1/\Delta_{\min}\} \epsilon_{\text{rad}} \Delta_{\max}$.

Proof Since $D_k = Q_k R_k$ has full-column rank, we have $D_k^\dagger = R_k^{-1} Q_k^\top$, that is, $R_k^{-1} = D_k^\dagger Q_k$. Therefore,

$$\left\| \widehat{R}_k^{-\top} \right\| = \left\| R_k^{-1} \right\| \overline{\text{diam}}(R_k) = \left\| D_k^\dagger Q_k \right\| \overline{\text{diam}}(R_k) \leq \left\| D_k^\dagger \right\| \overline{\text{diam}}(R_k) \leq M_{\widehat{R}^{-\top}}.$$

Notice that $\Delta_k \leq \overline{\text{diam}}(R_k) \leq \epsilon_{\text{rad}} \Delta_k \leq \epsilon_{\text{rad}} \Delta_{\text{max}}$. Applying all the above inequalities to Theorem 5, we see that $\widehat{m}_k(\widehat{s})$ belongs to a class of Q_k -fully quadratic models of f at x_k parameterized by $\Delta_k \in (0, \Delta_{\text{max}}]$ with constants κ_{ef}, κ_{eg} , and κ_{eh} . \square

Theorem 6 implies that \widehat{m}_k also belongs to a class of Q_k -fully linear models of f at x_k parameterized by $\Delta_k \in (0, \Delta_{\text{max}}]$ with constants κ_{ef} and κ_{eg} . As we explained at the beginning of this subsection, we will only use this fact in the convergence analysis of QARSTA in Section 3.

2.5 Subspace quality

In order to prove the convergence of our algorithm, in addition to model accuracy, we also need our subspaces to have a certain good quality, which we now describe. Inspired by [6], we introduce the notion of α -well aligned matrices.

Definition 8 *Given $f \in \mathcal{C}^1, x \in \mathbb{R}^n$, and $\alpha \in (0, 1)$, we say that $A \in \mathbb{R}^{n \times z}$ is α -well aligned for f at x if*

$$\|A^\top \nabla f(x)\| \geq \alpha \|\nabla f(x)\|.$$

In this subsection, we show that there exists $\alpha_D \in (0, 1)$ independent of k such that with nonzero probability each $D_k \in \mathbb{R}^{n \times p}$ constructed in QARSTA is α_D -well aligned for f at x_k . We begin by recalling one method to generate α -well aligned matrices with a certain probability from [15].

Theorem 7 *Suppose $\alpha, \delta_S \in (0, 1)$ and $z \geq 4(1 - \alpha)^{-2} \ln(1/\delta_S)$. Let $A \in \mathbb{R}^{n \times z}$ be a random matrix such that $A_{ij} \sim \mathcal{N}(0, 1/z)$. Then for any deterministic vector $v \in \mathbb{R}^n$,*

$$\mathbb{P} [\|A^\top v\| \geq \alpha \|v\|] \geq 1 - \delta_S.$$

In particular, given $f \in \mathcal{C}^1$ and $x \in \mathbb{R}^n$, A is α -well aligned for f at x with probability at least $1 - \delta_S$, i.e.,

$$\mathbb{P} [\|A^\top \nabla f(x)\| \geq \alpha \|\nabla f(x)\|] \geq 1 - \delta_S.$$

Proof See [15, Theorem 3.1, Corollary 3.1]. \square

In order to save function evaluations, in each iteration of QARSTA, only part of the matrix D_k is updated. As we explained in Subsection 2.3, this is done in order to maintain good geometry of the sample set. The updated matrix, generated according to Algorithm 4, comes from the QR -factorization of a random matrix A having the form described in Theorem 7. Thus we now explain how QR -factorization influences α -well alignedness.

The next lemma shows that, if matrix A is α -well aligned for f at x and has full-column rank, then the Q matrix from the QR -factorization is $(\alpha/\|A\|)$ -well aligned for f at x .

Lemma 4 *Suppose $f \in \mathcal{C}^1$ and let $x \in \mathbb{R}^n$. Let $\alpha \in (0, 1)$ and suppose that $A \in \mathbb{R}^{n \times z}$ is α -well aligned for f at x and has full-column rank. Let the QR -factorization of A be $A = QR$, where $Q \in \mathbb{R}^{n \times z}$ and $R \in \mathbb{R}^{z \times z}$. Then Q is $(\alpha/\|A\|)$ -well aligned for f at x .*

Proof Since A has full-column rank, we have $\|R\| = \|QR\| = \|A\| \neq 0$. Hence,

$$\alpha \|\nabla f(x)\| \leq \|A^\top \nabla f(x)\| \leq \|R^\top\| \|Q^\top \nabla f(x)\| = \|A\| \|Q^\top \nabla f(x)\|,$$

which implies

$$\|Q^\top \nabla f(x)\| \geq \frac{\alpha}{\|A\|} \|\nabla f(x)\|.$$

\square

Now we prove that there exists a constant $\alpha_D \in (0, 1)$ independent of k such that each $D_k \in \mathbb{R}^{n \times p}$ constructed in QARSTA is α_D -well aligned for f at x_k with probability at least $1 - \delta_S$.

We denote the randomly generated part of D_k by $D_k^R \in \mathbb{R}^{n \times q}$, where $p_{\text{rand}} \leq q \leq p$. This part is constructed by Algorithm 4. The unchanged part of D_k is denoted by $D_k^U \in \mathbb{R}^{n \times (p-q)}$. Hence, the matrix D_k has the form $D_k = [D_k^U \ D_k^R]$.

We require the following lemma, which gives a uniform bound on the norm of D_k^U .

Lemma 5 *Let $M_{D^U} = \epsilon_{\text{rad}} \Delta_{\text{max}} \sqrt{p}$. Then D_k^U satisfies $\|D_k^U\| \leq M_{D^U}$ for all k .*

Proof Notice that $D_k^U = [d_1^U \ \dots \ d_{p-q}^U] \in \mathbb{R}^{n \times (p-q)}$ is constructed by Algorithm 2 in the $(k-1)$ -st iteration. We have $\|d_i^U\| \leq \epsilon_{\text{rad}} \Delta_k$ for all $i = 1, \dots, p-q$. Consider $y = [y_1, \dots, y_{p-q}]^\top \in \mathbb{R}^{p-q}$. Using the AM-QM inequality, we get

$$\|D_k^U\| = \max_{\|y\|=1} \left\| \sum_{i=1}^{p-q} y_i d_i^U \right\| \leq \max_{1 \leq i \leq p-q} \|d_i^U\| \max_{\|y\|=1} \sum_{i=1}^{p-q} |y_i| \leq \epsilon_{\text{rad}} \Delta_k \sqrt{p-q} \leq M_{D^U}.$$

□

Theorem 8 *Suppose $f \in \mathcal{C}^1$. Suppose $\alpha, \delta_S \in (0, 1)$ and $q \geq 4(1-\alpha)^{-2} \ln(1/\delta_S)$. Suppose D_k^R is constructed by Algorithm 4 with $\Delta = \Delta_k$ and $M_A \geq 1$. Let*

$$\alpha_D = \min \left\{ \frac{\epsilon_{\text{geo}}^2}{M_{D^U}}, \frac{\alpha \Delta_{\text{min}}}{2M_A} \right\},$$

where $M_{D^U} = \epsilon_{\text{rad}} \Delta_{\text{max}} \sqrt{p}$. Then $D_k = [D_k^U \ D_k^R]$ is α_D -well aligned for f at x_k with probability at least $1 - \delta_S$.

Proof Let A be the matrix in Algorithm 4 with $A_{ij} \sim \mathcal{N}(0, 1/q)$, full-column rank, and $\|A\| \leq M_A$. For simplicity, we denote $g = \nabla f(x_k)$.

Case I: Suppose that in Algorithm 4 we set $\tilde{A} = A$.

According to Theorem 7, A is α -well aligned for f at x_k with probability at least $1 - \delta_S$. From Lemma 4, we have \tilde{Q} is $(\alpha/\|A\|)$ -well aligned for f at x_k . Notice that $D_k^R = \Delta_k \tilde{Q}$ and $\|A\| \leq M_A$. Thus we obtain

$$\|D_k^\top g\| \geq \left\| (D_k^R)^\top g \right\| = \Delta_k \left\| \tilde{Q}^\top g \right\| \geq \frac{\alpha \Delta_k}{\|A\|} \|g\| \geq \frac{\alpha \Delta_{\text{min}}}{M_A} \|g\| \geq \alpha_D \|g\|.$$

Case II: Suppose that in Algorithm 4 we set $\tilde{A} = A - QQ^\top A$, where Q is the orthonormal basis for the subspace determined by D_k^U .

Decompose g into $g = g_Q + g_{Q^\perp}$, where $g_Q = QQ^\top g$ is the projection of g onto the column space of Q and $g_{Q^\perp} = (I_n - QQ^\top)g$ is the projection of g onto the orthogonal complement of the column space of Q . Hence, we have $Q^\top g = Q^\top g_Q$ and $(I_n - QQ^\top)^\top g = (I_n - QQ^\top)g = g_{Q^\perp}$.

Applying Theorem 7 with $v = g_{Q^\perp}$, we have $\|A^\top g_{Q^\perp}\| \geq \alpha \|g_{Q^\perp}\|$ with probability at least $1 - \delta_S$. Notice that $D_k^R = \Delta_k \tilde{Q}$ and $\tilde{A} = (I_n - QQ^\top)A = \tilde{Q}\tilde{R}$. Thus we have $D_k^R = \Delta_k (I_n - QQ^\top)A\tilde{R}^{-1}$ which gives

$$\begin{aligned} \|D_k^\top g\| &= \sqrt{\left\| (D_k^U)^\top g \right\|^2 + \left\| (D_k^R)^\top g \right\|^2} \\ &= \sqrt{\left\| (D_k^U)^\top g_Q \right\|^2 + \Delta_k^2 \left\| \tilde{R}^{-\top} A^\top (I_n - QQ^\top)g \right\|^2} \\ &= \sqrt{\left\| (D_k^U)^\top g_Q \right\|^2 + \Delta_k^2 \left\| \tilde{R}^{-\top} A^\top g_{Q^\perp} \right\|^2}. \end{aligned} \tag{17}$$

Now we find lower bounds for each term under the square root symbol. Since the column space of Q is the same as the column space of D_k^U , there exists a vector $w \in \mathbb{R}^p$ such that $g_Q = D_k^U w$. Hence,

$$\left\| (D_k^U)^\top g_Q \right\| \geq \sigma_{\min} \left((D_k^U)^\top D_k^U \right) \|w\| = \sigma_{\min} (D_k^U)^2 \|w\| \geq \epsilon_{\text{geo}}^2 \|w\|,$$

where the first inequality comes from the fact that $\sigma_{\min}(M) = \min_{\|x\|=1} \|Mx\|$ for all square matrices M ([25, Theorem 3.1.2]) and the second inequality comes from Algorithm 2 and the fact that D_k^U must not be empty in this case (since Q is specified). Moreover, according to Lemma 5, we have $\|g_Q\| \leq \|D_k^U\| \|w\| \leq M_{D^U} \|w\|$ and so $\|w\| \geq \|g_Q\|/M_{D^U}$. Therefore,

$$\left\| (D_k^U)^\top g_Q \right\| \geq \frac{\epsilon_{\text{geo}}^2}{M_{D^U}} \|g_Q\|.$$

For the second term, we use the following inequality

$$\left\| \tilde{R}^\top \right\| = \left\| \tilde{R} \right\| = \left\| \tilde{A} \right\| = \left\| (I_n - QQ^\top)A \right\| \leq (\|I_n\| + \|QQ^\top\|) \|A\| \leq 2M_A$$

to get

$$\left\| \tilde{R}^{-\top} A^\top g_{Q^\perp} \right\| = \frac{\left\| \tilde{R}^\top \right\| \left\| \tilde{R}^{-\top} A^\top g_{Q^\perp} \right\|}{\left\| \tilde{R}^\top \right\|} \geq \frac{\left\| A^\top g_{Q^\perp} \right\|}{2M_A} \geq \frac{\alpha}{2M_A} \|g_{Q^\perp}\|.$$

Applying the above two lower bounds to (17), we have

$$\left\| D_k^\top g \right\| \geq \sqrt{\frac{\epsilon_{\text{geo}}^4}{(M_{D^U})^2} \|g_Q\|^2 + \Delta_k^2 \frac{\alpha^2}{4M_A^2} \|g_{Q^\perp}\|^2} \geq \alpha_D \sqrt{\|g_Q\|^2 + \|g_{Q^\perp}\|^2} = \alpha_D \|g\|,$$

which completes the proof. \square

3 Convergence analysis

In this section, we give the convergence analysis of the QARSTA algorithm. Our proof follows a general framework in [6]. However, since QARSTA uses different test conditions and a different class of models, our results are different from [6].

We note that there exists $M_D > 0$ such that all D_k satisfy $\|D_k\| \leq M_D$. To see this, suppose $D_k = [D_k^U \ D_k^R]$ where D_k^R is constructed by Algorithm 4 with $\Delta = \Delta_k$. Then we have $D_k^R = \Delta_k \tilde{Q}$ where \tilde{Q} consists of orthonormal columns and so $\|D_k^R\| = \Delta_k$. Hence,

$$\|D_k\| \leq \|D_k^U\| + \|D_k^R\| \leq M_{D^U} + \Delta_k \leq M_{D^U} + \Delta_{\max},$$

where M_{D^U} is defined in Lemma 5.

Suppose we have run $(K + 1)$ iterations and the stopping condition is not triggered, i.e., $\Delta_k \geq \Delta_{\min}$ for all $k \in \mathcal{K} = \{0, \dots, K\}$. We use the following subsets of \mathcal{K} :

- \mathcal{A} : the subset of \mathcal{K} where D_k is α_D -well aligned for f at x_k .
- \mathcal{A}^c : the subset of \mathcal{K} where D_k is not α_D -well aligned for f at x_k .
- \mathcal{C} : the subset of \mathcal{K} where the criticality test condition is satisfied.
- \mathcal{S} : the subset of \mathcal{K} where the criticality test condition is not satisfied with $\rho_k \geq \eta_1$.

We begin our analysis by introducing a few lemmas following [6].

Lemma 6 Suppose $f \in \mathcal{C}^{2+}$ with Lipschitz constant $L_{\nabla^2 f}$. Let $\epsilon > 0$. For all $k \in \mathcal{A} \setminus \mathcal{C}$ with $\|\nabla f(x_k)\| \geq \epsilon$, we have

$$\|\nabla \widehat{m}_k(\mathbf{0})\| \geq \epsilon_g(\epsilon),$$

where

$$\epsilon_g(\epsilon) = \frac{\alpha_D \epsilon}{(\kappa_{eg} \mu + 1) M_D} > 0.$$

Proof The criticality test condition is not satisfied, so we have $\Delta_k \leq \mu \|\nabla \widehat{m}_k(\mathbf{0})\|$. Notice that since \widehat{m}_k belongs to a class of Q_k -fully linear models of f at x_k , we get

$$\begin{aligned} \|Q_k^\top \nabla f(x_k)\| &\leq \|Q_k^\top \nabla f(x_k) - \nabla \widehat{m}_k(\mathbf{0})\| + \|\nabla \widehat{m}_k(\mathbf{0})\| \\ &\leq \kappa_{eg} \Delta_k + \|\nabla \widehat{m}_k(\mathbf{0})\| \\ &\leq (\kappa_{eg} \mu + 1) \|\nabla \widehat{m}_k(\mathbf{0})\|. \end{aligned}$$

Since D_k is α_D -well aligned for f at x_k , according to Lemma 4, Q_k is $(\alpha_D / \|D_k\|)$ -well aligned for f at x_k , so

$$\|Q_k^\top \nabla f(x_k)\| \geq \frac{\alpha_D}{\|D_k\|} \|\nabla f(x_k)\| \geq \frac{\alpha_D}{M_D} \|\nabla f(x_k)\| \geq \frac{\alpha_D}{M_D} \epsilon.$$

The result follows from combining the above inequalities. \square

For the remainder of this section, we make use of the following assumptions.

Assumption 1 Suppose $f \in \mathcal{C}^{2+}$ with Lipschitz constant $L_{\nabla^2 f}$.

Assumption 2 Suppose f is bounded below by f_{low} .

Assumption 3 Suppose $\|\nabla^2 \widehat{m}_k\| \leq \kappa_H$ for all k , where $\kappa_H \geq 1$ is independent of k .

Assumption 4 Suppose all solutions \widehat{s}_k of the trust-region subproblem satisfy

$$\widehat{m}_k(\mathbf{0}) - \widehat{m}_k(\widehat{s}_k) \geq c_1 \|\nabla \widehat{m}_k(\mathbf{0})\| \min \left(\Delta_k, \frac{\|\nabla \widehat{m}_k(\mathbf{0})\|}{\max \{\|\nabla^2 \widehat{m}_k\|, 1\}} \right),$$

for some $c_1 \in (0, 1/2]$ independent of k .

Assumption 5 Suppose each D_k is α_D -well aligned for f at x_k with probability at least $1 - \delta_S$, where α_D is independent of k .

We remark that under Assumption 1, as noted after Theorem 6, we have each \widehat{m}_k belongs to a class of Q_k -fully linear models of f at x_k parameterized by $\Delta_k \in (0, \Delta_{\max}]$ with constants κ_{ef} and κ_{eg} . Assumption 2 is standard for optimization. Using Assumption 1, Assumption 3 could alternatively be established by assuming f has compact level sets. Assumption 4 is always achievable by finding a sufficiently high-quality solution to the trust-region subproblem [4, 12]. Assumption 5 can be satisfied by setting p_{rand} , which is less than or equal to q , according to the lower bound on q required by Theorem 8.

Lemma 7 Suppose Assumptions 1 to 4 hold. Let $\epsilon > 0$. If $\|\nabla f(x_k)\| \geq \epsilon$ for all $k \in \mathcal{K}$, then

$$|\mathcal{A} \cap \mathcal{S}| \leq \phi(\epsilon),$$

where

$$\phi(\epsilon) = \frac{f(x^0) - f_{low}}{\eta_1 c_1 \epsilon_g(\epsilon) \min(\epsilon_g(\epsilon) / \kappa_H, \Delta_{\min})}$$

and $\epsilon_g(\epsilon)$ is defined in Lemma 6.

Proof See [6, Lemma 4] with $\Delta = \Delta_{\min}$. □

The following lemma bounds the remaining part of \mathcal{A} . We note that the proof is inspired by [6, Lemma 6].

Lemma 8 *The numbers of iterations in $\mathcal{A} \setminus \mathcal{S}$ and \mathcal{S} have the relation*

$$|\mathcal{A} \setminus \mathcal{S}| \leq C_1 |\mathcal{S}| + C_2,$$

where $C_1 = \ln(1/\gamma_{\text{dec}})^{-1} \ln(\gamma_{\text{inc}})$ and $C_2 = \ln(1/\gamma_{\text{dec}})^{-1} \ln(\Delta_0/\Delta_{\min})$.

Proof For all $k \in \mathcal{A} \setminus \mathcal{S}$, we have either the criticality test condition is satisfied, or the criticality test condition is not satisfied with $\rho_k < \eta_1$. In both cases, we have $\Delta_{k+1} = \gamma_{\text{dec}} \Delta_k$. For all $k \in \mathcal{S}$, we have $\Delta_{k+1} \leq \gamma_{\text{inc}} \Delta_k$.

Notice that Δ_k can only increase when $k \in \mathcal{S}$. Hence, the maximum Δ_k for all $k \in \mathcal{K}$ is bounded by $\Delta_0 \gamma_{\text{inc}}^{|\mathcal{S}|}$. Since the stopping condition is not triggered for all $k \in \mathcal{K}$, we must have

$$\Delta_0 \gamma_{\text{inc}}^{|\mathcal{S}|} \gamma_{\text{dec}}^{|\mathcal{A} \setminus \mathcal{S}|} \geq \Delta_{\min}.$$

Taking the natural logarithm of both sides, we get

$$\ln(\Delta_0) + \ln(\gamma_{\text{inc}}) |\mathcal{S}| + \ln(\gamma_{\text{dec}}) |\mathcal{A} \setminus \mathcal{S}| \geq \ln(\Delta_{\min}),$$

i.e.,

$$|\mathcal{A} \setminus \mathcal{S}| \leq \ln\left(\frac{1}{\gamma_{\text{dec}}}\right)^{-1} \ln(\gamma_{\text{inc}}) |\mathcal{S}| + \ln\left(\frac{1}{\gamma_{\text{dec}}}\right)^{-1} \ln\left(\frac{\Delta_0}{\Delta_{\min}}\right).$$

□

Combining Lemma 7 and 8, we get an upper bound for the cardinality of \mathcal{A} .

Lemma 9 *Suppose Assumptions 1 to 4 hold. Let $\epsilon > 0$. If $\|\nabla f(x_k)\| \geq \epsilon$ for all $k \in \mathcal{K}$, then we have*

$$|\mathcal{A}| \leq \psi(\epsilon) + \frac{C_1(K+1)}{C_1+1},$$

where $\psi(\epsilon) = \phi(\epsilon) + C_2/(C_1+1)$, $\phi(\epsilon)$ is defined in Lemma 7, and C_1 and C_2 are defined in Lemma 8.

Proof Using the Lemma 7 and 8, we obtain

$$\begin{aligned} |\mathcal{A}| &= |\mathcal{A} \cap \mathcal{S}| + |\mathcal{A} \setminus \mathcal{S}| \\ &\leq \phi(\epsilon) + C_1 |\mathcal{S}| + C_2 \\ &= \phi(\epsilon) + C_1 \left(|\mathcal{A} \cap \mathcal{S}| + |\mathcal{A}^{\text{G}} \cap \mathcal{S}| \right) + C_2 \\ &= \phi(\epsilon) + C_1 |\mathcal{A} \cap \mathcal{S}| + C_1 |\mathcal{A}^{\text{G}} \cap \mathcal{S}| + C_2 \\ &\leq (C_1+1)\phi(\epsilon) + C_1 |\mathcal{A}^{\text{G}}| + C_2 \\ &= (C_1+1)\phi(\epsilon) + C_1 ((K+1) - |\mathcal{A}|) + C_2 \\ &= (C_1+1)\phi(\epsilon) + C_1(K+1) - C_1 |\mathcal{A}| + C_2, \end{aligned}$$

which gives

$$|\mathcal{A}| \leq \phi(\epsilon) + \frac{C_1(K+1) + C_2}{C_1+1} = \psi(\epsilon) + \frac{C_1(K+1)}{C_1+1}.$$

□

The next Lemma is based on a general framework introduced in [21].

Lemma 10 *Suppose Assumption 5 holds. Then for all $\delta \in (0, 1)$, we have*

$$\mathbb{P}[|\mathcal{A}| \leq (1 - \delta)(1 - \delta_S)(K + 1)] \leq e^{-\delta^2(1 - \delta_S)(K + 1)/2}.$$

Proof See the proof of [6, Lemma 10 until inequality (67)]. Alternatively, [21, Lemma 4.5] with $p = 1 - \delta_S$, $\lambda = (1 - \delta)(1 - \delta_S)$, and $k = K + 1$. \square

Now we present our first convergence result, which gives a lower bound on the probability of finding a sufficiently small gradient in the first $(K + 1)$ iterations.

Theorem 9 *Suppose Assumptions 1 to 5 hold. Suppose $0 < \delta_S < 1/(C_1 + 1)$ with C_1 defined in Lemma 8. Let $\epsilon > 0$ and*

$$K \geq \frac{2\psi(\epsilon)}{1 - \delta_S - C_1/(C_1 + 1)} - 1,$$

where $\psi(\epsilon)$ is defined in Lemma 9. If the stopping condition is not triggered for all $k \in \{0, \dots, K\}$, then we have

$$\mathbb{P}\left[\min_{k \leq K} \|\nabla f(x_k)\| \leq \epsilon\right] \geq 1 - e^{-C_3(K+1)},$$

where

$$C_3 = \frac{(1 - \delta_S - C_1/(C_1 + 1))^2}{8(1 - \delta_S)}.$$

Proof Let $\epsilon_K = \min_{k \leq K} \|\nabla f(x_k)\|$ and $A_K = |\mathcal{A}|$. If $\epsilon_K = 0$, then $\min_{k \leq K} \|\nabla f(x_k)\| \leq \epsilon$ and we are done. If $\epsilon_K > 0$, then we have $A_K \leq \psi(\epsilon_K) + C_1(K + 1)/(C_1 + 1)$ by Lemma 9. Notice that $\psi(\cdot)$ is a non-increasing function and

$$\psi(\epsilon) \leq \frac{1}{2} \left(1 - \delta_S - \frac{C_1}{C_1 + 1}\right) (K + 1).$$

Therefore, we have

$$\begin{aligned} \mathbb{P}[\epsilon_K \geq \epsilon] &\leq \mathbb{P}[\psi(\epsilon_K) \leq \psi(\epsilon)] \\ &\leq \mathbb{P}\left[\psi(\epsilon_K) \leq \frac{1}{2} \left(1 - \delta_S - \frac{C_1}{C_1 + 1}\right) (K + 1)\right] \\ &\leq \mathbb{P}\left[A_K - \frac{C_1(K + 1)}{C_1 + 1} \leq \frac{1}{2} \left(1 - \delta_S - \frac{C_1}{C_1 + 1}\right) (K + 1)\right] \\ &= \mathbb{P}\left[A_K \leq \frac{1}{2} \left(1 - \delta_S + \frac{C_1}{C_1 + 1}\right) (K + 1)\right]. \end{aligned}$$

Since $\delta_S < 1/(C_1 + 1)$ and $C_1 > 0$, we have $1 - \delta_S > C_1/(C_1 + 1) > 0$, which gives

$$\frac{C_1}{(C_1 + 1)(1 - \delta_S)} \in (0, 1).$$

Hence, we can take

$$\delta = \frac{1}{2} \left[1 - \frac{C_1}{(C_1 + 1)(1 - \delta_S)}\right] \in (0, 1)$$

in Lemma 10 and obtain

$$\mathbb{P} \left[A_K \leq \frac{1}{2} \left(1 - \delta_S + \frac{C_1}{C_1 + 1} \right) (K + 1) \right] \leq e^{-C_3(K+1)}.$$

Therefore, we have

$$\mathbb{P} \left[\min_{k \leq K} \|\nabla f(x_k)\| \leq \epsilon \right] = 1 - \mathbb{P}[\epsilon_K \geq \epsilon] \geq 1 - e^{-C_3(K+1)}.$$

□

Based on Theorem 9, we get almost-sure liminf-type of convergence.

Theorem 10 *Suppose Assumptions 1 to 5 hold. Suppose $0 < \delta_S < 1/(C_1 + 1)$ with C_1 defined in Lemma 8. If QARSTA is run with $\Delta_{\min} = 0$, then*

$$\mathbb{P} \left[\inf_{k \geq 0} \|\nabla f(x_k)\| = 0 \right] = 1.$$

Proof Let $\epsilon > 0$ and

$$K \geq \frac{2\psi(\epsilon)}{1 - \delta_S - C_1/(C_1 + 1)} - 1, \tag{18}$$

where $\psi(\epsilon)$ is defined in Lemma 9. Notice that for all $\epsilon > 0$ and K satisfying (18) we have

$$\mathbb{P} \left[\inf_{k \geq 0} \|\nabla f(x_k)\| \leq \epsilon \right] \geq \mathbb{P} \left[\min_{k \leq K} \|\nabla f(x_k)\| \leq \epsilon \right] \geq 1 - e^{-C_3(K+1)},$$

where the second inequality comes from Theorem 9. Taking $K \rightarrow \infty$, we have for all $\epsilon > 0$,

$$\mathbb{P} \left[\inf_{k \geq 0} \|\nabla f(x_k)\| \leq \epsilon \right] \geq 1 - \lim_{K \rightarrow \infty} e^{-C_3(K+1)} = 1.$$

Finally, we take $\epsilon \rightarrow 0$ and use the continuity of probability to get

$$\mathbb{P} \left[\inf_{k \geq 0} \|\nabla f(x_k)\| = 0 \right] = 1.$$

□

We also have the expectation on the number of iterations used to find a sufficiently small gradient.

Theorem 11 *Suppose Assumptions 1 to 5 hold. Suppose $0 < \delta_S < 1/(C_1 + 1)$ with C_1 defined in Lemma 8. Let $\epsilon > 0$ and $K_\epsilon = \min \{k : \|\nabla f(x_k)\| \leq \epsilon\}$. Denote*

$$K_{\min}(\epsilon) = \frac{2\psi(\epsilon)}{1 - \delta_S - C_1/(C_1 + 1)} - 1,$$

where $\psi(\epsilon)$ is defined in Lemma 9. Then we have

$$\mathbb{E}[K_\epsilon] \leq K_{\min}(\epsilon) + \frac{e^{-C_3(K_{\min}(\epsilon)+1)}}{1 - e^{-C_3}} = \mathcal{O}(\epsilon^{-2}),$$

where C_3 is defined in Theorem 9.

Proof From Theorem 9, we have that for all $K \geq K_{\min}(\epsilon)$,

$$\mathbb{P}[K_\epsilon \leq K] = \mathbb{P}\left[\min_{k \leq K} \|f(x_k)\| \leq \epsilon\right] \geq 1 - e^{-C_3(K+1)}.$$

Notice that $\mathbb{E}[X] = \sum_{k=0}^{\infty} \mathbb{P}[X > k]$ for all non-negative integer-valued random variables X . Thus we obtain

$$\begin{aligned} \mathbb{E}[K_\epsilon] &= \sum_{K=0}^{K_{\min}(\epsilon)-1} \mathbb{P}[K_\epsilon > K] + \sum_{K=K_{\min}(\epsilon)}^{\infty} \mathbb{P}[K_\epsilon > K] \\ &\leq K_{\min}(\epsilon) + \sum_{K=K_{\min}(\epsilon)}^{\infty} e^{-C_3(K+1)} \\ &= K_{\min}(\epsilon) + \frac{e^{-C_3(K_{\min}(\epsilon)+1)}}{1 - e^{-C_3}}. \end{aligned}$$

The proof is complete by noticing that $K_{\min}(\epsilon) = \mathcal{O}(\epsilon^{-2})$. □

4 Numerical experiments

In this section, we develop numerical experiments to explore the performance of QARSTA. We select two sets of test problems from the CUTEst collection [19]. The dimension of each problem is between $n = 1000$ and $n = 1082$. In the first set, we select 73 unconstrained optimization problems with various forms of objective functions. This test set is chosen in order to compare the performance of QARSTA based on linear and quadratic approximation models. In the second set, we pick 32 unconstrained nonlinear least-squares problems, i.e.,

$$\min_{x \in \mathbb{R}^n} f(x) = \frac{1}{2} \|\mathbf{g}(x)\|^2 = \frac{1}{2} \sum_{i=1}^m g_i(x)^2,$$

where $\mathbf{g}(x) = [g_1(x), \dots, g_m(x)]^\top$ and $g_i(x) : \mathbb{R}^n \rightarrow \mathbb{R}$ for all $i = 1, \dots, m$. This set is chosen in order to demonstrate the advantages of exploring the structure of objective functions, which is a technique used in [6].

Our implementation of QARSTA is in Python 3, with random library `numpy.random` and trust-region subproblem solver `trsbox` from the DFBN algorithm implemented in [6]. The code is available upon request.

4.1 Results on general unconstrained problems

In order to demonstrate the advantages and disadvantages of using quadratic models, we compare the performance of QARSTA based on three sorts of models:

1. determined quadratic models $\widehat{m}(\widehat{s})$;
2. underdetermined quadratic models, constructed by a formula similar to $\widehat{m}(\widehat{s})$, with the model Hessian $\nabla_S^2 \widehat{f}(\mathbf{0}; R)$ replaced by

$$R^{-\top} \widetilde{\delta}_{\delta_f}(\mathbf{0}; R) R^{-1},$$

where the matrix $\widetilde{\delta}_{\delta_f}(\mathbf{0}; R)$ is given by setting all off-diagonal elements of $\delta_{\delta_f}(\mathbf{0}; R)$ to zero (see Equation (3) for definition of the δ_{δ_f} operator);

3. linear models, constructed by the formula

$$\tilde{m}(\hat{s}) = \hat{f}(\mathbf{0}) + \nabla_S \hat{f}(\mathbf{0}; R)^\top \hat{s},$$

which is the linear interpolation model of \hat{f} on the $(p + 1)$ points $\{\mathbf{0}\} \cup \{r_i : i = 1, \dots, p\}$.

The underdetermined quadratic model only uses function values in the form of $\hat{f}(\mathbf{0})$, $\hat{f}(r_i)$, and $\hat{f}(2r_i)$ where $i = 1, \dots, p$. Using a similar analysis technique as Theorems 1 and 2, it can be shown that the model constructed this way interpolates \hat{f} on all $(2p + 1)$ points $\{\mathbf{0}\} \cup \{r_i : i = 1, \dots, p\} \cup \{2r_i : i = 1, \dots, p\}$.

We note that all three models satisfy the convergence analysis shown in Section 3. Indeed, for determined quadratic models, we have proved in Subsection 2.4 that they are Q_k -fully quadratic and therefore Q_k -fully linear. For the other two models, notice that a full space linear interpolation model belongs to a class of fully linear models¹ [4, 12]. Since the underdetermined quadratic and linear models are at least as accurate as linear interpolation models, following a similar proof as in [4, 12] and Theorem 6 in this paper, it can be shown that they are Q_k -fully linear, which is sufficient for the results in Section 3.

For each of the three models, we consider $(p, p_{\text{rand}}) \in \{(1, 1), (10, 1), (10, 3), (10, 10)\}$. Hence, there are in total 12 variants of QARSTA to be compared. We note that among all 12 solvers, only the 6 solvers that have $p = 10$ and $p_{\text{rand}} \in \{3, 10\}$ are guaranteed to converge by our analysis in Section 3. Indeed, according to Theorems 8 to 11, we need $q \geq 4(1 - \alpha)^{-2} \ln(1/\delta_S)$ and $0 < \delta_S < 1/(C_1 + 1)$, where $\alpha \in (0, 1)$, $q \geq p_{\text{rand}}$ is the number of columns in D_k^R , and C_1 is defined in Lemma 8. In our implementation, we always set $\gamma_{\text{dec}} = 1/2$ and $\gamma_{\text{inc}} = 2$, which imply $C_1 = 1$. Letting $p_{\text{rand}} \geq 4(1 - \alpha)^{-2} \ln(1/\delta_S)$ with $0 < \alpha < 1$ and $0 < \delta_S < 1/2$, we get a lower bound $p_{\text{rand}} > 4 \ln 2 \approx 2.77$. Hence, the solvers with $p_{\text{rand}} \geq 3$ are guaranteed to converge by our convergence analysis. For solvers with $p_{\text{rand}} < 3$, our numerical results show that they still have a high probability of converging.

We use performance profiles [29] and data profiles [29] to present the results. The performance measure is either the number of function evaluations or runtime. For each test problem, we let x^* be the point that has the minimum objective function value obtained by all solvers within $100(n + 1)$ function evaluations. We regard a problem as successfully solved with accuracy level $\tau \in (0, 1)$ by a solver if, within $100(n + 1)$ function evaluations, there exists an iterate x_k such that

$$f(x_k) \leq f(x^*) + \tau (f(x_0) - f(x^*)),$$

where x_0 is the starting point. In the performance profile, we plot the proportion of test problems successfully solved by a solver against the ratio between the performance measure of that solver and the best performance measure of all solvers. In the data profiles, we plot the proportion of test problems successfully solved by a solver against the performance measure of that solver. For detailed explanations, see [29].

For clarity, for all profiles, we use the legend shown in Figure 1. We note that the data profiles based on runtime are truncated at 1 hour.

¹ In \mathbb{R}^n , this can be viewed as a class of I_n -fully linear models.

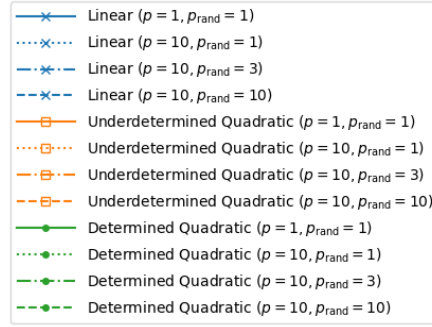


Fig. 1: Legend of figures.

4.1.1 Results based on runtime

Figures 2 and 3 present the performance and data profiles based on runtime with accuracy levels $\tau = 0.5$ and $\tau = 10^{-3}$. Figures 2 and 3 show that, for the low accuracy level $\tau = 0.5$, when measured by the runtime, solvers with $p = p_{\text{rand}} = 1$ perform better than other choices of p and p_{rand} . The solver based on determined quadratic models with $p = p_{\text{rand}} = 1$ is the best among all solvers. Moreover, solvers based on both sorts of quadratic models perform better than solvers based on linear models in general. For the high accuracy level $\tau = 10^{-3}$, we see a similar pattern when the runtime is small, but the solver based on underdetermined quadratic models with $p = 10$ and $p_{\text{rand}} = 10$ and linear models with $p = 10$ and $p_{\text{rand}} = 3$ solve more problem as runtime increases. As shown in Figure 3, within the 1-hour runtime budget, the solver based on underdetermined quadratic models with $p = 10$ and $p_{\text{rand}} = 10$ finally solves the most percentage of problems.

This implies that solvers based on quadratic models are generally more efficient than solvers based on linear models, and solvers with very small p and p_{rand} have the best efficiency. However, if the runtime is long enough, then solvers satisfying the convergence analysis have the potential to solve more problems. We should also note that our objective functions are very inexpensive to evaluate. Therefore, solvers based on quadratic models tend to have better performance on optimization problems where the objective function evaluations are inexpensive and quick solutions are preferred.

For completeness, the results with $\tau = 10^{-1}$ and $\tau = 10^{-2}$ can be found in Appendix A.

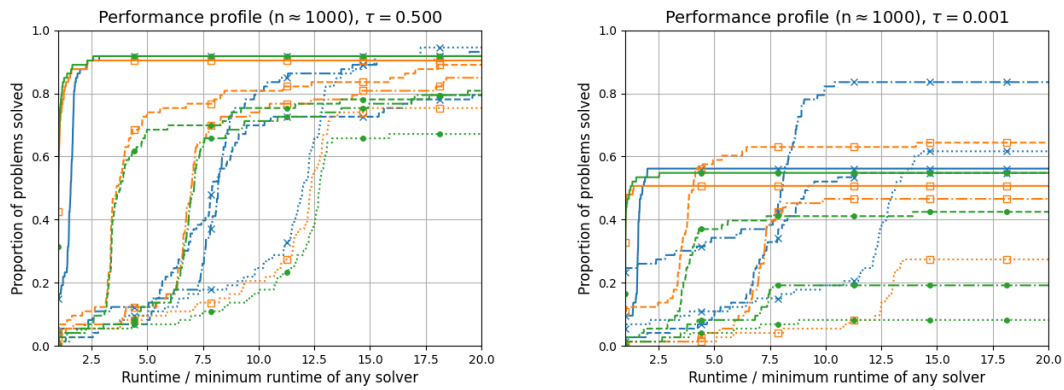


Fig. 2: Performance profiles with $\tau = 0.5$ and $\tau = 10^{-3}$ comparing the runtime.

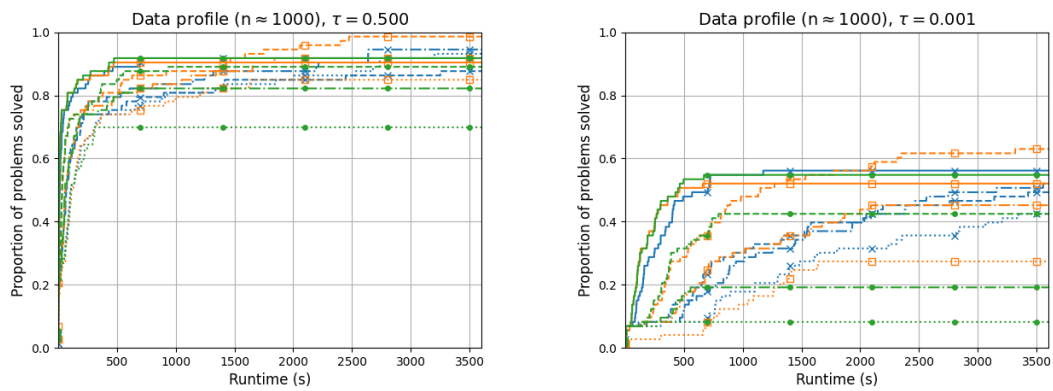


Fig. 3: Data profiles with $\tau = 0.5$ and $\tau = 10^{-3}$ comparing the runtime.

4.1.2 Results based on function evaluations

Figures 4 and 5 present the performance and data profiles based on function evaluations with accuracy levels $\tau = 0.5$ and $\tau = 10^{-3}$. We can see that when measured by function evaluations, for both low accuracy level $\tau = 0.5$ and high accuracy level $\tau = 10^{-3}$, solvers based on linear models perform better than other solvers in general, and the performance of solvers based on underdetermined models is better than solvers based on determined quadratic models in general.

This implies that although quadratic models are more accurate than linear models and thus may reduce the number of iterations required to reach a certain accuracy level, the increased number of function evaluations they need still makes the solvers take more overall function evaluations.

For completeness, the results with $\tau = 10^{-1}$ and $\tau = 10^{-2}$ can be found in Appendix A.

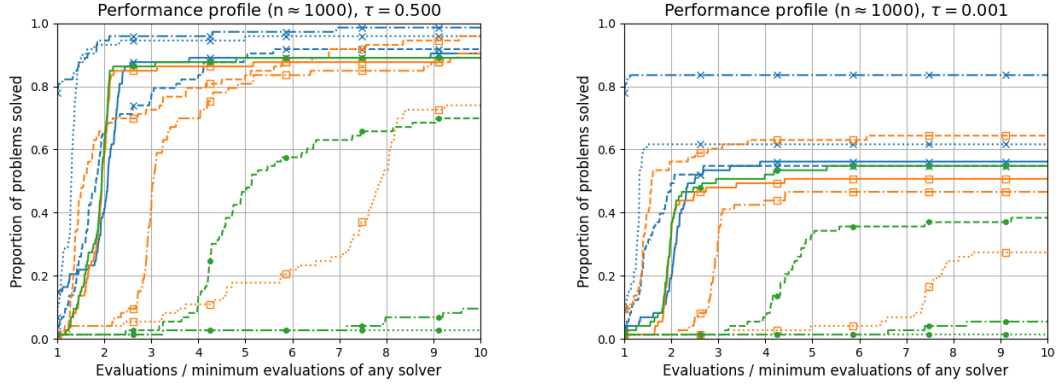


Fig. 4: Performance profiles with $\tau = 0.5$ and $\tau = 10^{-3}$ comparing the function evaluations.

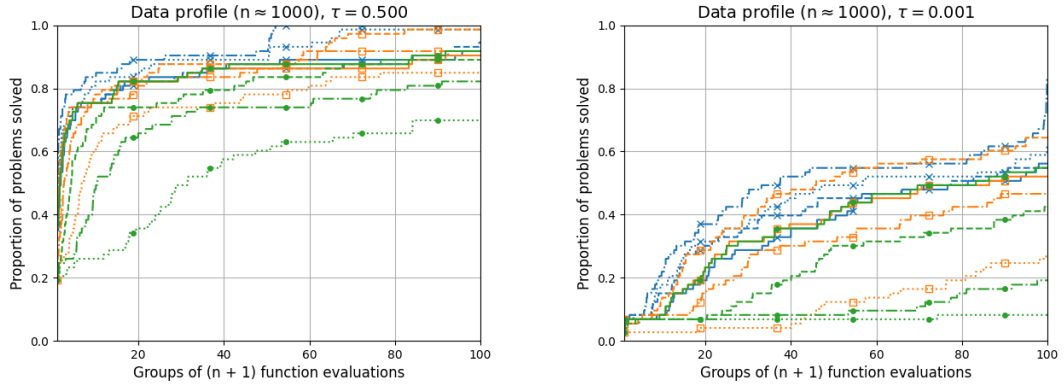


Fig. 5: Data profiles with $\tau = 0.5$ and $\tau = 10^{-3}$ comparing the function evaluations.

4.2 Results on nonlinear least-squares problems

For nonlinear least-squares problems, there exists another method to construct quadratic models. As shown in [6], we can first construct a subspace linear interpolation model for \mathbf{g} , denoted by $\tilde{m}_{\mathbf{g}}(\hat{\mathbf{s}})$, which interpolates $\hat{\mathbf{g}}(\hat{\mathbf{s}}) = \mathbf{g}(x^0 + Q\hat{\mathbf{s}})$ on the $(p+1)$ points $\{\mathbf{0}\} \cup \{r_i : i = 1, \dots, p\}$. Then we compute the square of the norm of $\tilde{m}_{\mathbf{g}}(\hat{\mathbf{s}})$ to get a quadratic model for \hat{f} . That is,

$$\hat{f}(\hat{\mathbf{s}}) \approx \frac{1}{2} \|\tilde{m}_{\mathbf{g}}(\hat{\mathbf{s}})\|^2.$$

We note that the quadratic models constructed by this method may not interpolate \hat{f} on more than $(p+1)$ points. However, it can be shown that they are Q_k -fully linear and therefore satisfy the convergence analysis in Section 3. The proof can be found in [6] or by applying the theory of model functions operations developed in [9].

In this set of experiments, we compare the performance of QARSTA based on the model mentioned above and the three models described in Subsection 4.1. The results are presented by

performance profiles [29] and data profiles [29] with the same parameters as in Subsection 4.1. For all the profiles, we use the legend shown in Figure 1 plus the following new labels.

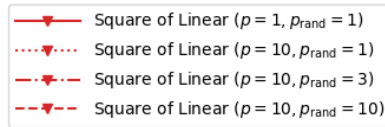


Fig. 6: Legend of figures (continued).

4.2.1 Results based on runtime

Figures 7 and 8 present the performance and data profiles based on runtime with accuracy levels $\tau = 0.5$ and $\tau = 10^{-3}$. Figures 7 and 8 show that, for the low accuracy level $\tau = 0.5$, when measured by the runtime, solvers based on square-of-linear models perform better than linear models, but worse than other quadratic models in general. However, for the high accuracy level $\tau = 10^{-3}$, the solver based on square-of-linear models with $p = p_{\text{rand}} = 10$ is significantly better than other solvers, which agrees with past results found in [6]. This implies that exploring the structure of objective functions increases the efficiency of solvers, especially for high accuracy levels.

For completeness, the results with $\tau = 10^{-1}$ and $\tau = 10^{-2}$ can be found in Appendix A.

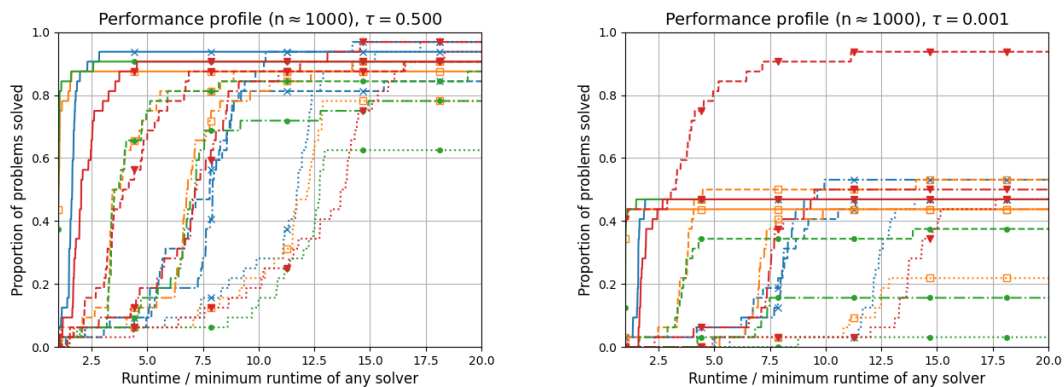


Fig. 7: Performance profiles with $\tau = 0.5$ and $\tau = 10^{-3}$ comparing the runtime.

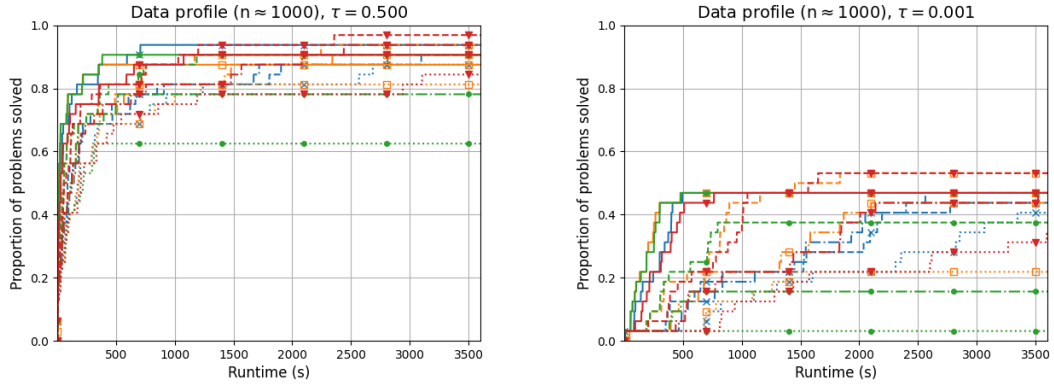


Fig. 8: Data profiles with $\tau = 0.5$ and $\tau = 10^{-3}$ comparing the runtime.

4.2.2 Results based on function evaluations

Figures 9 and 10 present the performance and data profiles based on function evaluations with accuracy levels $\tau = 0.5$ and $\tau = 10^{-3}$. When measured by function evaluations, as shown in Figures 9 and 10, for both accuracy levels $\tau = 0.5$ and $\tau = 10^{-3}$, the solvers based on square-of-linear models perform the best in general. Once again, the solver based on square-of-linear models with $p = p_{\text{rand}} = 10$ is significantly better than other solvers and agrees with past results found in [6]. This again demonstrates the advantage of exploring the structure of objective functions.

For completeness, the results with $\tau = 10^{-1}$ and $\tau = 10^{-2}$ can be found in Appendix A.

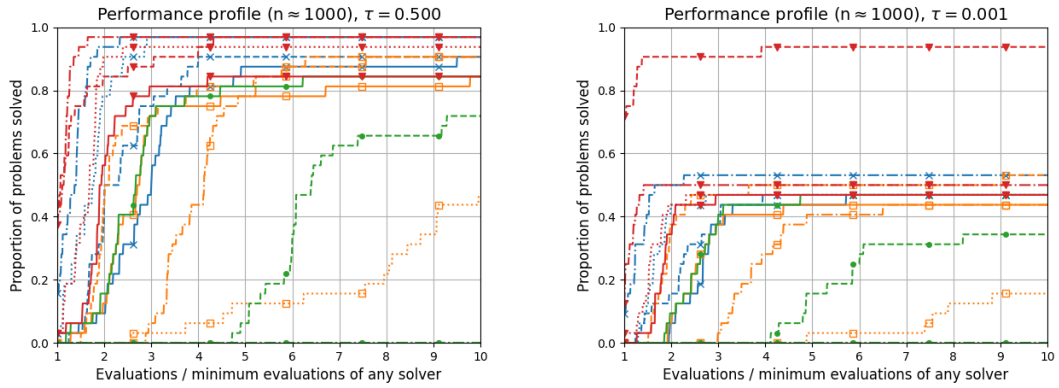


Fig. 9: Performance profiles with $\tau = 0.5$ and $\tau = 10^{-3}$ comparing the function evaluations.

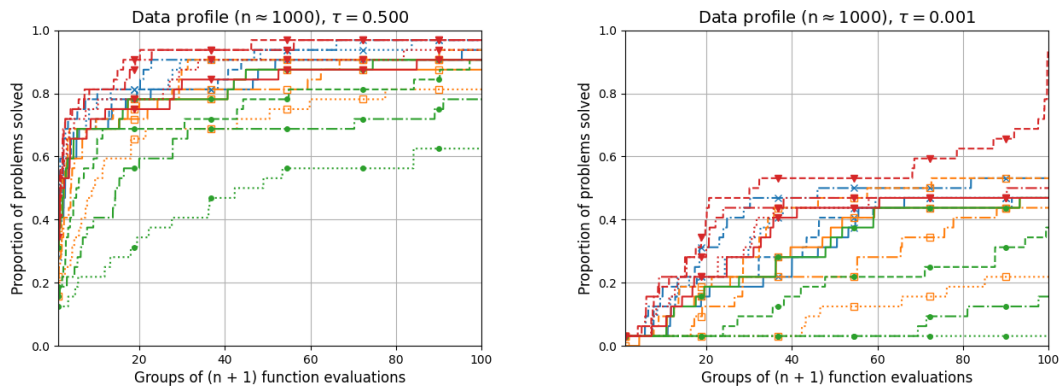


Fig. 10: Data profiles with $\tau = 0.5$ and $\tau = 10^{-3}$ comparing the function evaluations.

5 Conclusion

In this paper, we proposed QARSTA, a random subspace derivative-free trust-region algorithm for unconstrained deterministic optimization problems. This algorithm extends the previous random subspace trust-region algorithms to a much broader scope by using quadratic approximation models instead of linear models and getting rid of the requirement that the problems take a certain form (e.g., nonlinear least-squares). We provided theoretical guarantees for QARSTA including model accuracy, sample set geometry, and subspace quality. In particular, we provided a Q -fully quadratic modeling technique that is easy to handle in both theoretical analysis and computer programming aspects. Based on a framework introduced in [6], we proved the almost-sure global convergence of QARSTA and gave an expected result on the number of iterations required to reach a certain accuracy. Numerical results demonstrated the efficiency of using quadratic models over linear models in QARSTA and the benefits of exploring the structure of objective functions when possible.

In addition, most of the theoretical results in this paper can be applied more broadly to other DFO analyses, as they do not depend on the given algorithm. In particular, we note that Subsections 2.1 and 2.4 provide a new method to construct Q -fully quadratic models, which is more accurate than required by the framework in [6] and the convergence analysis in this paper. Subsections 2.3 and 2.5 provide theoretical guarantees for the sample set management procedure and the subspace updating procedure used in this paper. These results can also be extended to provide theoretical guarantees for some of the procedures used in [6]. For example, Theorem 4 provides a theoretical explanation for the direction-generating mechanism used in [6, Algorithm 5]. Subsection 2.5 shows how the choice of p_{rand} , QR -factorization, and matrix enhancement influence α -well alignedness, which are not clearly explained in [6].

A More numerical results

A.1 Results on general unconstrained problems

A.1.1 Results based on runtime

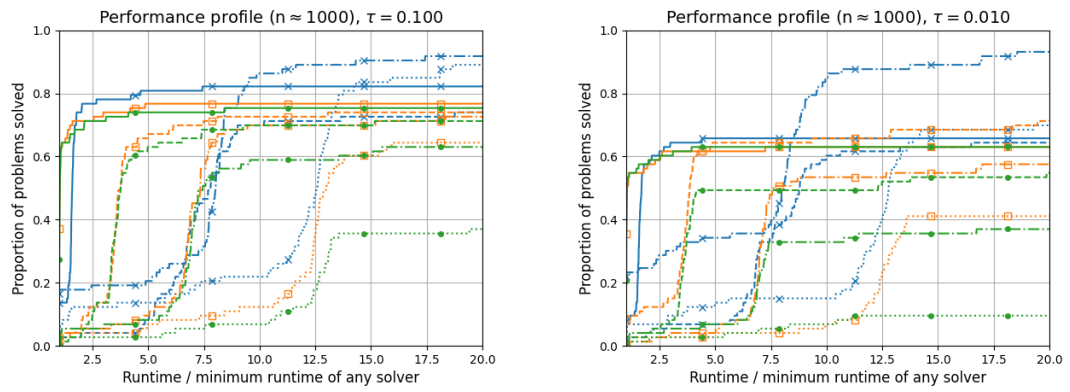


Fig. 11: Performance profiles with $\tau = 10^{-1}$ and $\tau = 10^{-2}$ comparing the runtime.

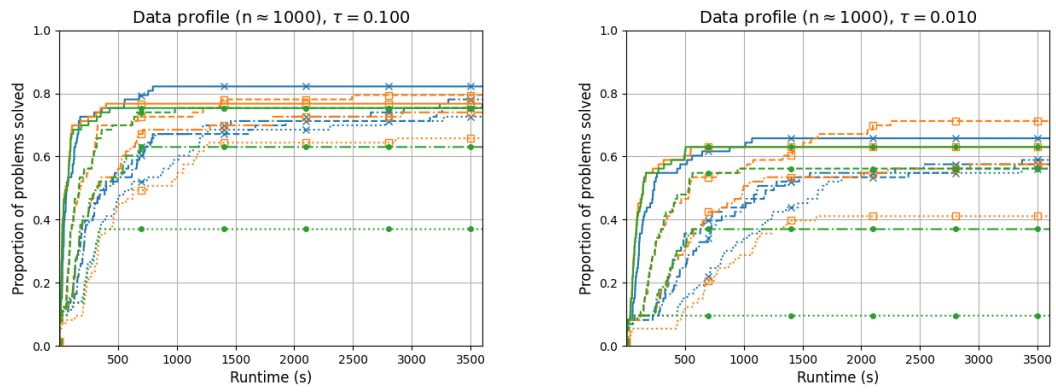


Fig. 12: Data profiles with $\tau = 10^{-1}$ and $\tau = 10^{-2}$ comparing the runtime.

A.1.2 Results based on function evaluations

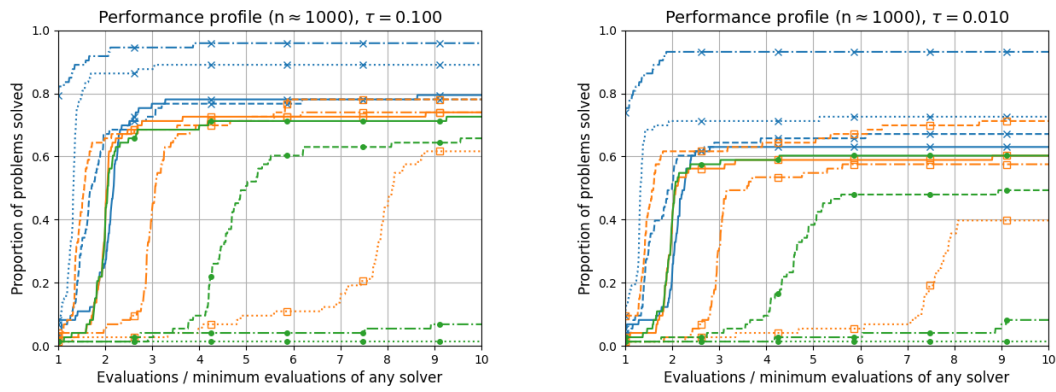


Fig. 13: Performance profiles with $\tau = 10^{-1}$ and $\tau = 10^{-2}$ comparing the function evaluations.

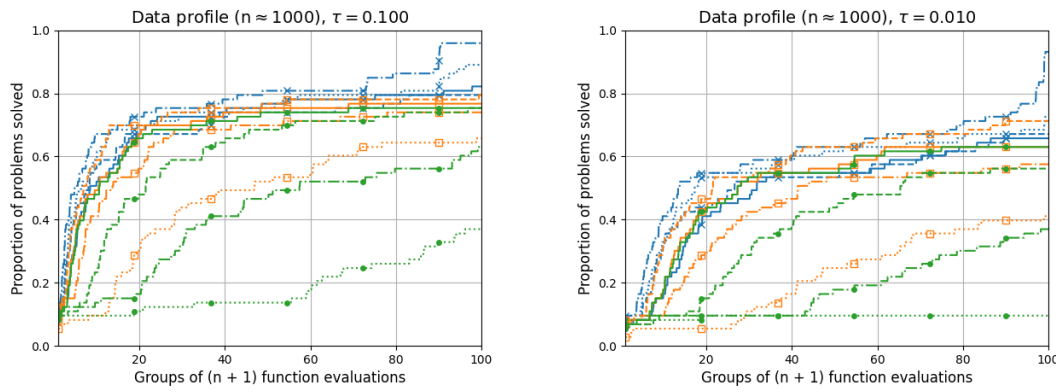


Fig. 14: Data profiles with $\tau = 10^{-1}$ and $\tau = 10^{-2}$ comparing the function evaluations.

A.2 Results on nonlinear least-squares problems

A.2.1 Results based on runtime

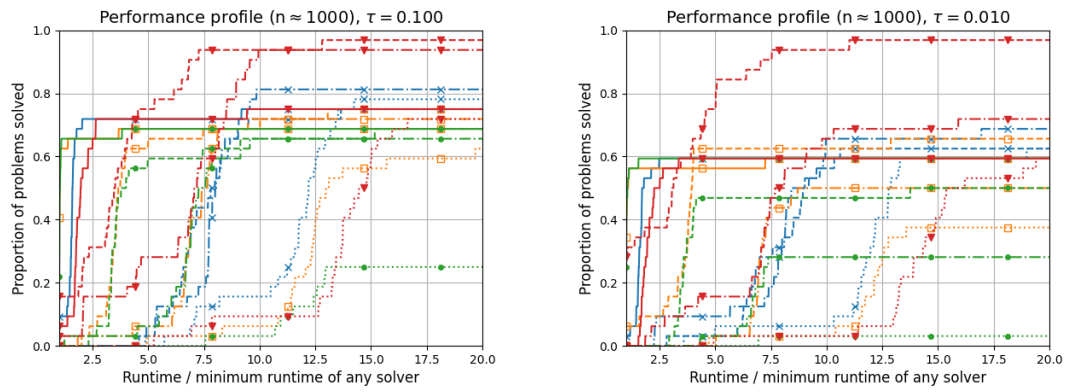


Fig. 15: Performance profiles with $\tau = 10^{-1}$ and $\tau = 10^{-2}$ comparing the runtime.

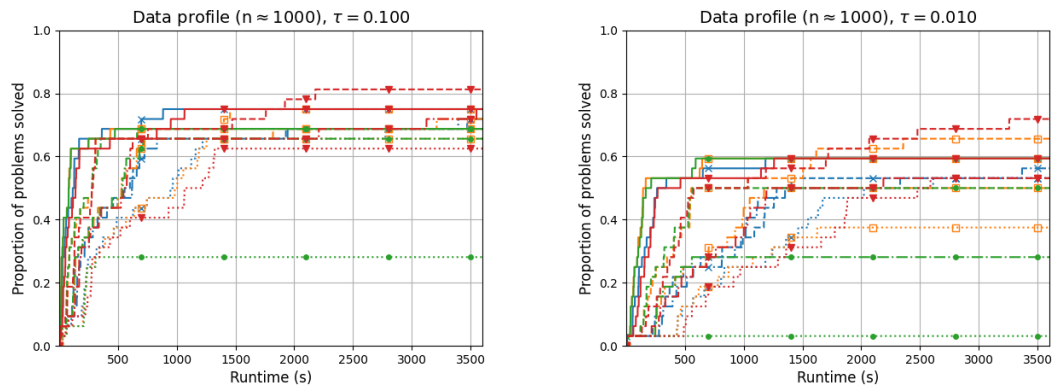


Fig. 16: Data profiles with $\tau = 10^{-1}$ and $\tau = 10^{-2}$ comparing the runtime.

A.2.2 Results based on function evaluations

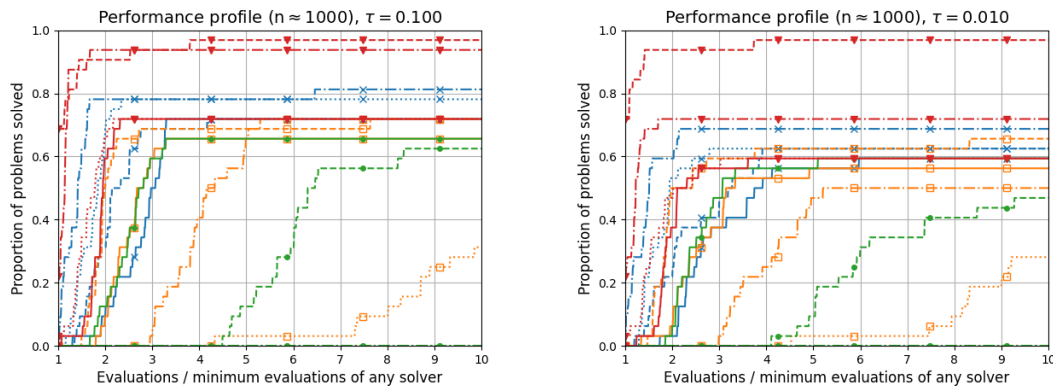


Fig. 17: Performance profiles with $\tau = 10^{-1}$ and $\tau = 10^{-2}$ comparing the function evaluations.

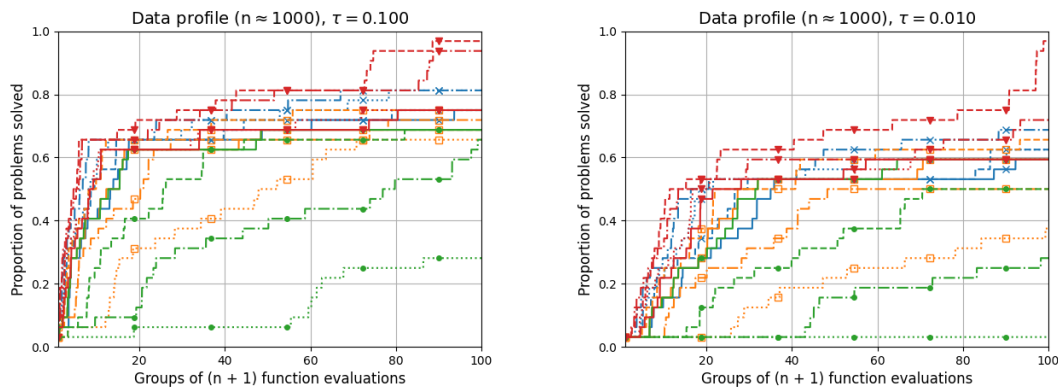


Fig. 18: Data profiles with $\tau = 10^{-1}$ and $\tau = 10^{-2}$ comparing the function evaluations.

References

1. S. ALARIE, C. AUDET, A. E. GHERIBI, M. KOKKOLARAS, AND S. LE DIGABEL, *Two decades of blackbox optimization applications*, EURO J. Comput. Optim., 9 (2021), p. 100011.
2. M. ALZANTOT, Y. SHARMA, S. CHAKRABORTY, H. ZHANG, C. HSIEH, AND M. B. SRIVASTAVA, *GenAttack: practical black-box attacks with gradient-free optimization*, in Proceedings of the Genetic and Evolutionary Computation Conference, 2019, pp. 1111–1119.
3. C. AUDET, J. E. DENNIS JR, AND S. LE DIGABEL, *Parallel space decomposition of the mesh adaptive direct search algorithm*, SIAM J. Optim., 19 (2008), pp. 1150–1170.
4. C. AUDET AND W. HARE, *Derivative-free and blackbox optimization*, Springer, Cham, 2017.
5. ———, *Model-based methods in derivative-free nonsmooth optimization*, Springer, Cham, 2020, pp. 655–691.
6. C. CARTIS AND L. ROBERTS, *Scalable subspace methods for derivative-free nonlinear least-squares optimization*, Math. Program., 199 (2023), pp. 461–524.
7. P. CHEN, H. ZHANG, Y. SHARMA, J. YI, AND C. HSIEH, *ZOO: zeroth order optimization based black-box attacks to deep neural networks without training substitute models*, in Proceedings of the 10th ACM Workshop on Artificial Intelligence and Security, 2017, pp. 15–26.
8. Y. CHEN AND W. HARE, *Adapting the centred simplex gradient to compensate for misaligned sample points*, IMA J. Numer. Anal., (2023).

9. Y. CHEN, W. HARE, AND G. JARRY-BOLDUC, *Error analysis of surrogate models constructed through operations on submodels*, Math. Oper. Res., (2022).
10. A. CONN, K. SCHEINBERG, AND L. N. VICENTE, *Geometry of interpolation sets in derivative free optimization*, Math. Program., 111 (2008), pp. 141–172.
11. ———, *Geometry of sample sets in derivative-free optimization: polynomial regression and underdetermined interpolation*, IMA J. Numer. Anal., 28 (2008), pp. 721–748.
12. ———, *Introduction to derivative-free optimization*, SIAM, 2009.
13. A. CONN, P. L. TOINT, A. SARTENAER, AND N. GOULD, *On iterated-subspace minimization methods for nonlinear optimization*, tech. rep., Rutherford Appleton Laboratory, 1994.
14. J. E. DENNIS JR. AND R. B. SCHNABEL, *Numerical methods for unconstrained optimization and nonlinear equations*, SIAM, 1996.
15. K. J. DZAHINI AND S. M. WILD, *Stochastic trust-region algorithm in random subspaces with convergence and expected complexity analyses*, (2022). [arXiv:2207.06452](https://arxiv.org/abs/2207.06452).
16. M. FEURER AND F. HUTTER, *Hyperparameter optimization*, Springer, Cham, 2019, pp. 3–33.
17. M. FUKUSHIMA, *Parallel variable transformation in unconstrained optimization*, SIAM J. Optim., 8 (1998), pp. 658–672.
18. H. GHANBARI AND K. SCHEINBERG, *Black-box optimization in machine learning with trust region based derivative free algorithm*, (2017). [arXiv:1703.06925](https://arxiv.org/abs/1703.06925).
19. N. GOULD, D. ORBAN, AND P. L. TOINT, *CUTEst: a constrained and unconstrained testing environment with safe threads for mathematical optimization*, Comput. Optim. Appl., 60 (2015), pp. 545–557.
20. G. N. GRAPIGLIA, J. YUAN, AND Y. YUAN, *A subspace version of the Powell–Yuan trust-region algorithm for equality constrained optimization*, J. Oper. Res. Soc. China, 1 (2013), pp. 425–451.
21. S. GRATTON, C. W. ROYER, L. N. VICENTE, AND Z. ZHANG, *Direct search based on probabilistic descent*, SIAM J. Optim., 25 (2015), pp. 1515–1541.
22. W. HARE AND G. JARRY-BOLDUC, *Calculus identities for generalized simplex gradients: rules and applications*, SIAM J. Optim., 30 (2020), pp. 853–884.
23. W. HARE, G. JARRY-BOLDUC, AND C. PLANIDEN, *A matrix algebra approach to approximate hessians*, IMA J. Numer. Anal., (2023).
24. W. HARE, L. ROBERTS, AND C. W. ROYER, *Expected decrease for derivative-free algorithms using random subspaces*, (2023). [arXiv:2308.04734](https://arxiv.org/abs/2308.04734).
25. R. A. HORN AND C. R. JOHNSON, *Topics in matrix analysis*, Cambridge University Press, 1991.
26. J. LARSON, M. MENICKELLY, AND S. M. WILD, *Derivative-free optimization methods*, Acta Numer., 28 (2019), pp. 287–404.
27. Z. LI, F. LIU, W. YANG, S. PENG, AND J. ZHOU, *A survey of convolutional neural networks: analysis, applications, and prospects*, IEEE Trans. Neural Netw. Learn. Syst., (2021).
28. G. LIUZZI, S. LUCIDI, F. RINALDI, AND L. N. VICENTE, *Trust-region methods for the derivative-free optimization of nonsmooth black-box functions*, SIAM J. Optim., 29 (2019), pp. 3012–3035.
29. J. J. MORÉ AND S. M. WILD, *Benchmarking derivative-free optimization algorithms*, SIAM J. Optim., 20 (2009), pp. 172–191.
30. R. PENROSE, *A generalized inverse for matrices*, in Mathematical Proceedings of the Cambridge Philosophical Society, vol. 51, Cambridge University Press, 1955, pp. 406–413.
31. M. J. D. POWELL, *The NEWUOA software for unconstrained optimization without derivatives*, Springer US, Boston, MA, 2006, pp. 255–297.
32. ———, *Developments of NEWUOA for minimization without derivatives*, IMA J. Numer. Anal., 28 (2008), pp. 649–664.
33. ———, *The BOBYQA algorithm for bound constrained optimization without derivatives*, tech. rep., University of Cambridge, 2009.
34. L. ROBERTS AND C. W. ROYER, *Direct search based on probabilistic descent in reduced spaces*, SIAM J. Optim., 33 (2023), pp. 3057–3082.
35. Z. ZHANG, *On derivative-free optimization methods (in Chinese)*, PhD thesis, Chinese Academy of Sciences, 2012. <https://www.zhangzk.net/docs/publications/thesis.pdf>.